tortoise (*Gopherus agassizii*; figure 1). Distributed north and west of the Colorado River, the species was listed as *threatened* under the US Endangered Species Act in 1990. Because of its protected status, Agassiz's desert tortoise acts as an "umbrella species," extending protection to other plants and animals within its range (Tracy and Brussard, 1994). The newly described Morafka's desert tortoise (*Gopherus morafkai*; Murphy et al. 2011) is another species of significant conservation concern in the desert Southwest, found east of the Colorado River. Both tortoises are important as ecological engineers who construct burrows that provide shelter to many other animal species, which allows them to escape the temperature extremes of the desert (Ernst and Lovich 2009). The importance of these tortoises is thus greatly disproportionate to their intrinsic value as species. By virtue of their protected status, Agassiz's desert tortoises have a significant impact on regulatory issues in the listed portion of their range, yet little is known about the effects of USSEDO on the species, even a quarter century after the recognition of that deficiency (Pearson 1986). Large areas of habitat occupied by Agassiz's desert tortoise in particular have potential for development of USSED (figure 2).

Figure 1. Agassiz's desert tortoise (*Gopherus agassizii*). Large areas of desert tortoise habitat are developed or being evaluated for renewable energy development, including for wind and solar energy. Photograph: Jeffrey E. Lovich.

In this article, we review the state of knowledge about the known and potential effects, both direct and indirect, of USSEDO on wildlife (table 1). Our review is based on information published primarily in peer-reviewed scientific journals for both energy and wildlife professionals. Agassiz's desert tortoise is periodically highlighted in our review because of its protected status, wide distribution in areas considered for USSEDO in the desert Southwest, and well-studied status (Ernst and Lovich 2009). In addition, we identify gaps in our understanding of the effects of USSEDO on wildlife and suggest questions that will guide future research toward a goal of mitigating or minimizing the negative effects on wildlife.

Background on proposed energy-development potential in the southwestern United States

The blueprint for evaluating and permitting the development of solar energy on public land in the region, as is required under the US National Environmental Policy Act (USEPA 2010), began in a draft environmental impact statement (EIS) prepared by two federal agencies (USDOI and USDOE 2011a). The purpose of the EIS is to "develop a new Solar Energy Program to further support utility-scale solar energy development on BLM [US Bureau of Land

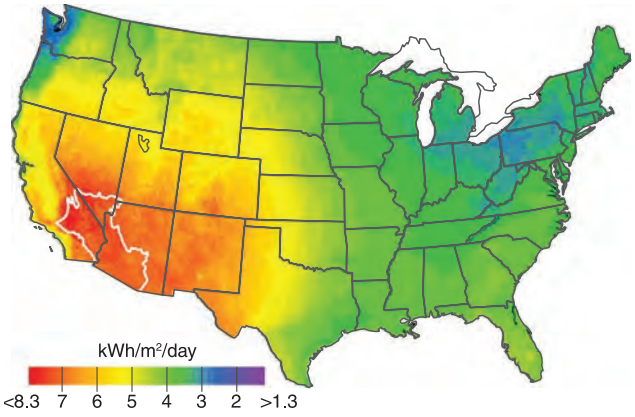

Figure 2. Concentrating solar energy potential (in kilowatt-hours per square meter per day [kWh/m²/day]) of the United States. The map shows the annual average direct normal solar resource data based on a 10-kilometer satellite-modeled data set for the period from 1998 to 2005. Refer to NREL (2011) for additional details and data sources. The white outline defines the approximate composite ranges of Agassiz's (west of the Colorado River) and Morafka's (east of the Colorado River) desert tortoises (Murphy et al. 2011) in the United States, both species of significant conservation concern. This figure was prepared by the National Renewable Energy Laboratory for the US Department of Energy (NREL 2011). The image was authored by an employee of the Alliance for Sustainable Energy, LLC, under Contract no. DE-AC36-08GO28308 with the US Department of Energy. Reprinted with permission from NREL 2011.

Table 1. List of known and potential impacts of utility-scale solar energy development on wildlife in the desert Southwest.

Impacts due to facility construction and decommissioning	Impacts due to facility presence, operation, and maintenance
Destruction and modification of wildlife habitat	Habitat fragmentation and barriers to movement and gene flow
Direct mortality of wildlife	Noise effects
Dust and dust-suppression effects	Electromagnetic field effects
Road effects	Microclimate effects
Off-site impacts	Pollution effects from spills
Destruction and modification of wildlife habitat	Water consumption effects
	Fire effects
	Light pollution effects, including polarized light
	Habitat fragmentation and barriers to movement and gene flow
	Noise effects

Management] -administered lands… and to ensure consistent application of measures to avoid, minimize, or mitigate the adverse impacts of such development" (p. ES-2). As of February 2010, the BLM had 127 active applications for solar facilities on lands that the BLM administers. According to USDOI and USDOE (2011a), all of the BLM-administered land in six states (California, Arizona, Utah, Nevada, New Mexico, and Colorado) was considered initially, for a total of 178 million hectares (ha). Not all of that land is compatible with solar energy development, so three alternative configurations are listed by USDOI and USDOI (2011a) for consideration, ranging from 274,244 to 39,972,558 ha. The larger figure is listed under the *no action alternative* where BLM would continue to use existing policy and guidance to evaluate applications. Of the area being considered under the two action alternatives, approximately 9 million ha meet the criteria established under the BLM's preferred action alternative to support solar development. Twenty-five criteria were used to exclude certain areas of public land from solar development and include environmental, social, and economic factors. The preferred alternative also included the identification of proposed *solar energy zones* (SEZs), defined as "area[s] with few impediments to utility-scale production of solar energy" (USDOI and USDOE 2011a, p. ES-7). By themselves, these SEZs constitute the nonpreferred action alternative of 274,244 ha listed above. Maps of SEZs are available at *http://solareis.anl.gov/documents/dpeis/index.cfm*.

Several sensitive, threatened, or endangered species are being considered within the EIS, but Agassiz's desert tortoise is one of only four species noted whose very presence at a site may be sufficient to exclude USSED in special cases (see table ES.2-2 in USDOI and USDOE 2011a). The potential effects of USSEDO are not trivial for tortoises or other wildlife species. Within the area covered in the draft EIS by USDOI and USDOE (2011a), it is estimated that approximately 161,943 ha of Agassiz's desert tortoise habitat will be directly affected. However, when including direct and indirect impacts on habitat (excluding transmission lines and roads that would add additional impacts; see Lovich and Bainbridge 1999, Kristan and Boarman 2007), it is estimated that approximately 769,230 ha will be affected. Some SEZs are adjacent to critical habitat designated for the recovery of Agassiz's desert tortoise, and this proximity is considered part of the indirect impacts.

On 28 October 2011, while this paper was in press, the BLM and US Department of Energy released a supplement to the EIS (USDOI and USDOE 2011b, 2011c) after receiving more than 80,500 comments. The no action alternative remains the same as in the EIS. The new preferred alternative (slightly reduced to 8,225,179 ha as the modified program alternative) eliminates or adjusts SEZs (now reduced to 115,335 ha in 17 zones as the modified SEZ alternative) to ensure that they are not in high-conflict areas and provides incentives for their use. The new plan also proposes a process to accommodate additional solar energy development outside of SEZs and to revisit ongoing state-based planning efforts to allow consideration of additional SEZs in the future.

The impacts of USSED on wildlife: Effects due to construction and decommissioning

The construction and eventual decommissioning of solar energy facilities will have impacts on wildlife, including rare and endangered species, and on their habitats in the desert (Harte and Jassby 1978). These activities involve significant ground disturbance and direct (e.g., mortality) and indirect (e.g., habitat loss, degradation, modification) impacts on wildlife and their habitat (Kuvlesky et al. 2007). Solar energy facilities require large land areas to harness sunlight and convert it to electrical energy. According to Wilshire and colleagues (2008), photovoltaic panels with a 10% conversion efficiency would need to cover an area of about 32,000 square kilometers, or an area a little smaller than the state of Maryland, to meet the current electricity demands of the United States. Many of the areas being considered for the development of solar energy in the Mojave and Sonoran Deserts are, at present, relatively undisturbed (USDOI and USDOE 2011a).

The extent of surface disturbance of USSED is related to the cooling technology used. Because of the scarcity of water in the desert Southwest region, dry-cooling systems, which consume 90%–95% less water than wet-cooling systems (EPRI 2002), are becoming a more viable option for concentrating solar facilities. Although wet-cooling systems are more economical and efficient, they consume larger amounts of water per kilowatt-hour (Torcellini et al. 2003). Unlike wet-cooling systems, dry-cooling systems use ambient air, instead of water, to cool the exhaust steam from the turbines. However, to achieve a heat-rejection efficiency similar to that in a wet-cooling system, Khalil and colleagues (2006) estimated that a direct dry-cooling system will require a larger footprint and would thus affect more wildlife habitat.

Although we found no information in the scientific literature about the direct effects of USSED on wildlife, the ground-disturbance impacts are expected to be similar to those caused by other human activities in the desert (Lovich and Bainbridge 1999).

Dust and dust suppressants. USSED transforms the landscape substantially through site preparation, including the construction of roads and other infrastructure. In addition, many solar facilities require vegetation removal and grading. These construction activities produce dust emissions, especially in arid environments (Munson et al. 2011), which already have the potential for natural dust emission. Dust can have dramatic effects on ecological processes at all scales (reviewed by Field et al. 2010). At the smallest scale, wind erosion, which powers dust emission, can alter the fertility and water-retention capabilities of the soil. Physiologically, dust can adversely influence the gas exchange, photosynthesis, and water usage of Mojave Desert shrubs (Sharifi et al. 1997). Depending on particle size, wind speed, and other factors, dust emission can physically damage plant species through root exposure, burial, and abrasions to their leaves and stems. The physiological and physical damage to plant species inflicted by dust emissions could ultimately reduce the plants' primary production and could indirectly affect wildlife food plants and habitat quality.

From an operational perspective, dust particles reduce mirror and panel efficiency in converting solar energy into heat or electricity. To combat dust, solar energy facilities apply various dust suppressants to surfaces with exposed soil (e.g., graded areas, areas with vegetation removed, roads). There are eight categories of common dust suppressants used for industrial applications: water, salts and brines, organic nonpetroleum products, synthetic polymers, organic petroleum, electrochemical substances, clay additives, and mulch and fiber mixtures (reviewed in Piechota et al. 2004). In a study conducted in the Mojave Desert in which the hydrological impacts of dust suppressants were compared, Singh and colleagues (2003) reported that changes did occur in the volume, rate, and timing of runoff when dust suppressants were used. In particular, petroleum-based and acrylic-polymer dust suppressants drastically influenced the hydrology of disturbed areas by increasing runoff volume and changing its timing. When it is applied to disturbed desert soils, magnesium chloride ($MgCl_2$), a commonly used salt-based dust depressant, does not increase runoff volume but does, however, increase the total suspended solids loads in runoff (Singh et al. 2003).

Others have highlighted the fact that there is a dearth of scientific research and literature on the effects of dust suppressants on wildlife, including the most commonly used category of dust depressant: brines and salts (Piechota et al. 2004, Goodrich et al. 2008). However, the application of $MgCl_2$ to roads was correlated with a higher frequency of plant damage (Goodrich et al. 2008). Because chloride salts, including $MgCl_2$, are not confined to the point of application but have the ability to be transported in runoff (White and Broadly 2001), the potential exists for a loss of primary production associated with plant damage in the habitats surrounding a solar facility, which could directly affect wildlife habitat.

Mortality of wildlife. We are not aware of any published studies documenting the direct effects of USSED on the survival of wildlife. However, subterranean animals can be affected by USSED, including species that hibernate underground. In the Sonoran Desert portion of California, Cowles (1941) observed that most reptiles in the Coachella Valley hibernated at depths of less than 33 centimeters (cm), with many at considerably shallower depths. Included in his observations were flat-tailed horned lizards (*Phrynosoma mcallii*)—a species of special concern in the region because of solar energy development (USDOI and USDOE 2011a)—and the federally protected Coachella Valley fringe-toed lizard (*Uma inornata*). Even lightweight vehicles like motorcycles are capable of causing greatly increased soil density (soil compaction) at a depth of 30–60 cm as their tires pass over the surface (Webb 1983). These observations suggest that vehicular activities in the desert have the potential to kill or entrap large numbers of subterranean animals (Stebbins 1995) through compressive forces or burrow collapse. Similar or greater impacts would be expected from the heavy equipment associated with the construction activities at an energy facility.

Destruction and modification of wildlife habitat. Despite the absence of published, peer-reviewed information on the effects of USSED on wildlife and their habitats, a considerable body of literature exists on the effects of other ground-disturbing activities on both ecological patterns and processes that are broadly comparable. Ground-disturbing activities affect a variety of processes in the desert, including soil density, water infiltration rate, vulnerability to erosion, secondary plant succession, invasion by exotic plant species, and stability of cryptobiotic soil crusts (for reviews, see Lovich and Bainbridge 1999, Webb et al. 2009). All of these processes have the ability—individually and together—to alter habitat quality, often to the detriment of wildlife. Any disturbance and alteration to the desert landscape, including the construction and decommissioning of utility-scale solar energy facilities, has the potential to increase soil erosion. Erosion can physically and physiologically affect plant species and can thus adversely influence primary production (Sharifi et al. 1997, Field et al. 2010) and food availability for wildlife.

Solar energy facilities require substantial site preparation (including the removal of vegetation) that alters topography and, thus, drainage patterns to divert the surface flow associated with rainfall away from facility infrastructure (Abbasi and Abbasi 2000). Channeling runoff away from plant communities can have dramatic negative effects on water availability and habitat quality in the desert, as was shown by Schlesinger and colleagues (1989). Areas deprived

of runoff from sheet flow support less biomass of perennial and annual plants relative to adjacent areas with uninterrupted water-flow patterns.

The impacts of roads. Roads are required in order to provide access to solar energy infrastructure. Both paved and unpaved roads have well-documented negative effects on wildlife (Forman and Alexander 1998), and similar effects are expected in utility-scale solar energy facilities. Although road mortality is most easily detected on the actual roadway, the effects of roads extend far beyond their physical surface. In a study of the effects of roads on Agassiz's desert tortoise populations in southern Nevada, von Seckendorff Hoff and Marlow (2002) examined transects along roads with traffic volumes varying from 25 to 5000 vehicles per day. Tortoises and tortoise sign (e.g., burrows, shells, scat) decreased with their proximity to a road. On roads with high traffic volumes, tortoises and tortoise sign were reduced as far as 4000 meters from the roadside. Roads with lower traffic volumes had fewer far-reaching effects.

Another effect of roads in the desert is the edge enhancement of plants and arthropod herbivores (Lightfoot and Whitford 1991). Perennial plants along the roadside are often larger than those farther away, and annual plant germination is often greatest along the shoulders of roads. It is possible that increased runoff due to impervious pavement or compacted soil contributes to this heterogeneity of vegetation in relationship to a road. Agassiz's desert tortoises may select locations for burrow construction that are close to roads, perhaps because of this increased productivity of food plants (Lovich and Daniels 2000). Although this situation suggests potentially beneficial impacts for herbivorous species of wildlife, such as tortoises, it increases their chance of being killed by vehicle strikes, as was shown by von Seckendorff Hoff and Marlow (2002).

Off-site impacts. Direct impacts on wildlife and habitat can occur well outside the actual footprint of the energy facility. Extraction of large amounts of raw materials for the construction of solar energy facilities (e.g., aggregate, cement, steel, glass); transportation and processing of those materials; the need for large amounts of water for cooling some installations; and the potential for the production of toxic wastes, including coolants, antifreeze, rust inhibitors, and heavy metals, can affect wildlife adjacent to or far from the location of the facility (Abbasi and Abbasi 2000). Abbasi and Abbasi (2000) summarized data suggesting that the material requirements for large-scale solar facilities exceed those for conventional fossil-fuel plants on a cost-per-unit-of-energy basis. In addition, water used for steam production at one solar energy facility in the Mojave Desert of California contained selenium, and the wastewater was pumped into evaporation ponds that attracted birds that fed on invertebrates. Although selenium toxicity was not considered a threat on the basis of the results of one study, the possibility exists for harmful bioaccumulation of this toxic micronutrient (Herbst 2006). In recognition of the hazard, Pimentel and colleagues (1994) suggested that fencing should be used to keep wildlife away from these toxic ponds.

The impacts of USSED on wildlife: Effects due to operation and maintenance

This category includes the effects related to the presence and operation of the solar facility, not the physical construction and decommissioning of the same. Some of the effects (e.g., mortality of wildlife and impacts caused by roads) are similar to those discussed previously for construction and decommissioning and are not discussed further.

Habitat fragmentation. Until relatively recently, the desert Southwest was characterized by large blocks of continuous and interconnected habitat. Roads and urban development continue to contribute to habitat fragmentation in this landscape. Large-scale energy development has the potential to add to and exacerbate the situation, presenting potential barriers to movement and genetic exchange in wildlife populations, including those of bighorn sheep (*Ovis canadensis*), deer (*Odocoileus* spp.), tortoises, and other species of concern and social significance. Research conducted on the effects of oil and gas exploration and development (OGED) on wildlife in the Intermountain West provides a possible analog to USSEDO, since comparable data are not available for the desert Southwest. The potential effects on mule deer (*Odocoileus hemionus*) and other wildlife species include impediments to free movement, the creation of migration bottlenecks, and a reduction in effective winter range size. Mule deer responded immediately to OGED by moving away from disturbances, with no sign of acclimation during the three years of study by Sawyer and colleagues (2009). Some deer avoidance resulted in their use of less-preferred and presumably less-suitable habitats.

Despite a lack of data on the direct contributions of USSEDO to habitat fragmentation, USSEDO has the potential to be an impediment to gene flow for some species. Although the extent of this impact is, as yet, largely unquantified in the desert, compelling evidence for the effects of human-caused habitat fragmentation on diverse wildlife species has already been demonstrated in the adjacent coastal region of southern California (Delaney et al. 2010).

Noise effects. Industrial noise can have impacts on wildlife, including changes to their habitat use and activity patterns, increases in stress, weakened immune systems, reduced reproductive success, altered foraging behavior, increased predation risk, degraded communication with conspecifics, and damaged hearing (Barber et al. 2009, Pater et al. 2009). Changes in sound level of only a few decibels can elicit substantial animal responses. Most noise associated with USSEDO is likely to be generated during the construction phase (Suter 2002), but noise can also be produced during operation and maintenance activities. Brattstrom and Bondello (1983) documented the effects of noise on Mojave

Desert wildlife on the basis of experiments involving off-highway vehicles. Noise from some of these vehicles can reach 110 decibels—near the threshold of human pain and certainly within the range expected for various construction, operation, and maintenance activities (Suter 2002) associated with USSEDO. This level of noise caused hearing loss in animals, such as kangaroo rats (*Dipodomys* spp.), desert iguanas (*Dipsosaurus dorsalis*), and fringe-toed lizards (*Uma* spp.). In addition, it interfered with the ability of kangaroo rats to detect predators, such as rattlesnakes (*Crotalus* spp.), and caused an unnatural emergence of aestivating spadefoot toads (*Scaphiopus* spp.), which would most likely result in their deaths. Because of impacts on wildlife, Brattstrom and Bondello (1983) recommended that "all undisturbed desert habitats, critical habitats, and all ranges of threatened, endangered, or otherwise protected desert species" (p. 204) should be protected from loud noise.

Although many consider solar energy production a "quiet" endeavor, noise is associated with their operation. For example, facilities at which wet-cooling systems are used will have noises generated by fans and pumps. As for facilities with dry-cooling systems, only noise from fans will be produced during operation (EPRI 2002). Because of the larger size requirements of dry-cooling systems, there will be more noise production associated with an increase in the number of fans.

Electromagnetic field generation. When electricity is passed through cables, it generates electric and magnetic fields. USSEDO requires a large distribution system of buried and overhead cables to transmit energy from the point of production to the end user. Electromagnetic fields (EMFs) produced as energy flows through system cables are a concern from the standpoint of both human and wildlife health, yet little information is available to assess the potential impact of the EMFs associated with USSEDO on wildlife. Concerns about EMFs have persisted for a long time, in part because of controversy over whether they're the actual cause of problems and disagreement about the underlying mechanisms for possible effects. For example, there is presently a lack of widely accepted agreement about the biological mechanisms that can explain the consistent associations between extremely low-frequency EMF exposure from overhead power lines and childhood leukemia, although there is no shortage of theories (Gee 2009).

Some conclude that the effects of EMFs on wildlife will be minor because of reviews of the often conflicting and inconclusive literature on the topic (Petersen and Malm 2006). Others suggest that EMFs are a possible source of harm for diverse species of wildlife and contribute to the decline of some mammal populations. Balmori (2010) listed possible impacts of chronic exposure to athermal electromagnetic radiation, which included damage to the nervous system, disruption of circadian rhythm, changes in heart function, impairment of immunity and fertility, and genetic and developmental problems. He concluded that enough evidence exists to confirm harm to wildlife but suggested that further study is urgently needed. Other authors suggest that the generally inconsistent epidemiological evidence in support of the effects of EMFs should not be cause for inaction. Instead, they argue that the precautionary principle should be applied in order to prevent a recurrence of the "late lessons from early warnings" scenario that has been repeated throughout history (Gee 2009).

Magnetic information is used for orientation by diverse species, from insects (Sharma and Kumar 2010) to reptiles (Perry A et al. 1985). Despite recognition of this phenomenon, the direct effects of USSEDO-produced EMFs on wildlife orientation remains unknown.

Microclimate effects. The alteration of a landscape through the removal of vegetation and the construction of structures by humans not only has the potential of increasing animal mortality but also changes the characteristics of the environment in a way that affects wildlife. The potential for microclimate effects unique to solar facilities was discussed by Pimentel and colleagues (1994) and by Harte and Jassby (1978). It has been estimated that a concentrating solar facility can increase the albedo of a desert environment by 30%–56%, which could influence local temperature and precipitation patterns through changes in wind speed and evapotranspiration. Depending on their design, large concentrating solar facilities may also have the ability to produce significant amounts of unused heat that could be carried downwind into adjacent wildlife habitat with the potential to create localized drought conditions. The heat produced by central-tower solar facilities can burn or incinerate birds and flying insects as they pass through the concentrated beams of reflected light (McCrary et al. 1986, Pimentel et al. 1994, Tsoutsos et al. 2005, Wilshire et al. 2008).

A dry-cooled solar facility—in particular, one with a concentrating-trough system—could reject heated air from the cooling process with temperatures 25–35 degrees Fahrenheit higher than the ambient temperature (EPRI 2002). This could affect the microclimate on site or those in adjacent habitats. To our knowledge, no research is available to assess the effects of USSEDO on temperature or that of any other climatic variable on wildlife. However, organisms whose sex is determined by incubation temperatures, such as both species of desert tortoises, may be especially sensitive to temperature changes, because small temperature changes have the potential to alter hatchling sex ratios (Hulin et al. 2009).

Pollutants from spills. USSEDO, especially at wet-cooled solar facilities, has a potential risk for hazardous chemical spills on site, associated with the toxicants used in cooling systems, antifreeze agents, rust inhibitors, herbicides, and heavy metals (Abbasi and Abbasi 2000, Tsoutsos et al. 2005). Wet-cooling solar systems must use treatment chemicals (e.g., chlorine, bromine, selenium) and acids and bases (e.g., sulfuric acid, sodium hydroxide, hydrated lime) for the prevention of fouling and scaling and for pH control of the water used in their recirculating systems (EPRI 2002).

Solar facilities at which a recirculating system is used also have treatment and disposal issues associated with water discharge, known as *blowdown*, which is water with a high concentration of dissolved and suspended materials created by the numerous evaporation cycles in the closed system (EPRI 2002). These discharges may contain chemicals used to prevent fouling and scaling. The potentially tainted water is usually stored in evaporative ponds, which further concentrates the toxicants (Herbst 2006). Because water is an attraction for desert wildlife, numerous species could be adversely affected. The adverse effects of the aforementioned substances and similar ones on wildlife are well documented in the literature, and a full review is outside the scope of this article. However, with the decreased likelihood of wet-cooling systems for solar facilities in the desert, the risk of hazardous spills and discharges on site will be less in the future, because dry-cooling systems eliminate most of the associated water-treatment processes (EPRI 2002). However, there are still risks of spills associated with a dry-cooling system. More research is needed on the adverse effects of chemical spills and tainted-water discharges specifically related to USSEDO on wildlife.

Water consumption (wet-cooled solar). The southwestern United States is a water-poor region, and water use is highly regulated throughout the area. Because of this water limitation, the type of cooling systems installed at solar facilities is limited as well. For example, a once-through cooling system—a form of wet cooling—is generally not feasible in arid environments, because there are few permanent bodies of water (i.e., rivers, oceans, and lakes) from which to draw cool water and then into which to release hot water. Likewise, other wet-cooling options, such as recirculating systems and hybrid systems, are becoming less popular because of water shortage issues in the arid region. Therefore, the popularity of the less-efficient and less-economical dry-cooling systems is increasing on public lands. Water will also be needed at solar facilities to periodically wash dust from the mirrors or panels. Although there are numerous reports in which the costs and benefits were compared both environmentally and economically (EPRI 2002, Khalil et al. 2006) between wet- and dry-cooled solar facilities, to our knowledge no one has actually quantified the effects of water use and consumption on desert wildlife in relation to the operation of these facilities.

Fire risks. Any system that produces electricity and heat has a potential risk of fire, and renewable energy facilities are no exception. Concentrating solar energy facilities harness the sun's energy to heat oils, gases, or liquid sodium, depending on the system design (e.g., heliostat power, trough, dish). With temperatures reaching more than 300 degrees Celsius in most concentrated solar systems, spills and leaks from the coolant system increase the risk of fires (Tsoutsos et al. 2005). Even though all vegetation is usually removed from the site during construction, which reduces the risk of a fire propagating on and off site, the increase of human activity in a desert region increases the potential for fire, especially along major highways and in the densely populated western Mojave Desert (Brooks and Matchett 2006).

The Southwest deserts are not fire-adapted ecosystems: fire was historically uncommon in these regions (Brooks and Esque 2002). However, with the establishment of numerous flammable invasive annual plants in the desert Southwest (Brown and Minnich 1986), coupled with an increase in anthropogenic ignitions, fire has become more common in the deserts, which adversely affects wildlife (Esque et al. 2003). For Agassiz's desert tortoise, fire can translate into direct mortality at renewable energy facilities (Lovich and Daniels 2000) and can cause reductions in food and habitat quality. To our knowledge, however, there is no scientific literature related to the effects of USSEDO-caused fire on wildlife.

Light pollution. Two types of light pollution could be produced by solar energy facilities: ecological light pollution (ELP; Longcore and Rich 2004) and polarized light pollution (PLP; Horváth et al. 2009). The latter, PLP, could be produced at high levels at facilities using photovoltaic solar panels, because dark surfaces polarize light. ELP can also be produced at solar facilities in the form of reflected light. The reflected light from USSEDO has been suggested as a possible hazard to eyesight (Abbasi and Abbasi 2000). ELP could adversely affect the physiology, behavior, and population ecology of wildlife, which could include the alteration of predation, competition, and reproduction (for reviews, see Longcore and Rich 2004, Perry G et al. 2008). For example, the foraging behavior of some species can be adversely affected by light pollution (for a review, see Longcore and Rich 2004). The literature is limited regarding the impact of artificial lighting on amphibians and reptiles (Perry G et al. 2008), and, to our knowledge, there are no published studies in which the impacts on wildlife of light pollution produced by USSEDO have been assessed. However, light pollution is considered by G. Perry and colleagues (2008) to be a serious threat to reptiles, amphibians, and entire ecological communities that requires consideration during project planning. G. Perry and colleagues (2008) further recommended the removal of unnecessary lighting so that the lighting conditions of nearby habitats would be as close as possible to their natural state.

Numerous anthropogenic products—usually those that are dark in color (e.g., oil spills, glass panes, automobiles, plastics, paints, asphalt roads)—can unnaturally polarize light, which can have adverse effects on wildlife (for a review, see Horváth et al. 2009). For example, numerous animal species use polarized light for orientation and navigation purposes (Horváth and Varjú 2004). Therefore, the potential exists for PLP to disrupt the orientation and migration abilities of desert wildlife, including those of sensitive species. In the review by Horváth and colleagues (2009), which was focused mostly on insects but included a few avian references, they highlighted the fact that anthropogenic products that produce PLP can appear to be water bodies to wildlife and can become ecological traps for insects and, to a lesser degree, avian species. Therefore,

utility-scale solar energy facilities at which photovoltaic technology is used in the desert Southwest could create a direct effect on insects (i.e., ecological trap), which could have profound but unquantified effects on the ecological community surrounding the solar facility. In addition, there may be indirect effects on wildlife through the limitation of plant food resources, especially if pollinators are negatively affected. As was stated by Horváth and colleagues (2009), the population- and community-level effects of PLP can only be speculated on because of the paucity of data.

Unanswered questions and research needs

In our review of the peer-reviewed scientific literature, we found only one peer-reviewed publication on the specific effects of utility-scale solar energy facility operation on wildlife (McCrary et al. 1986) and none on utility-scale solar energy facility construction or decommissioning. Although it is possible that we missed other peer-reviewed publications, our preliminary assessment demonstrates that very little critically reviewed information is available on this topic. The dearth of published, peer-reviewed scientific information provides an opportunity to identify the fundamental research questions for which resource managers need answers. Without those answers, resource managers will be unable to effectively minimize the negative effects of USSEDO on wildlife, especially before permitting widespread development of this technology on relatively undisturbed public land.

Before-and-after studies. Carefully controlled studies are required in order to tease out the direct and indirect effects of USSEDO on wildlife. Pre- and postconstruction evaluations are necessary to identify the effects of renewable energy facilities and to compare results across studies (Kunz et al. 2007). In their review of wind energy development and wildlife, with an emphasis on birds, Kuvlesky and colleagues (2007) noted that experimental designs and data-collection standards were typically inconsistent among studies. This fact alone contributes measurably to the reported variability among studies or renders comparisons difficult, if not impossible. Additional studies should emphasize the need for carefully controlled before-after-control-impact (BACI) studies (Kuvlesky et al. 2007) with replication (if possible) and a detailed description of site conditions. The potential payoff for supporting BACI studies now could be significant: They could provide answers for how to mitigate the negative impacts on wildlife in a cost-effective and timely manner.

What are the cumulative effects of large numbers of dispersed or concentrated energy facilities? Large portions of the desert Southwest have the potential for solar energy development. Although certain areas are targeted for large facilities because of resource availability and engineering requirements (e.g., their proximity to existing transmission corridors), other areas may receive smaller, more widely scattered facilities. A major unanswered question is what the cumulative impacts of these facilities on wildlife are. Would it be better for wildlife if development is concentrated or if it is scattered in smaller, dispersed facilities? Modeling based on existing data would be highly suspect because of the deficiency of detailed site-level published information identified in our analysis. Except for those on habitat destruction and alteration related to other human endeavors, there are no published articles on the population genetic consequences of habitat fragmentation related to USSED, which makes this a high priority for future research.

What density or design of development maximizes energy benefits while minimizing negative effects on wildlife? We are not aware of any published peer-reviewed studies in which the impacts on wildlife of different USSED densities or designs have been assessed. For example, would it benefit wildlife to leave strips of undisturbed habitat between rows of concentrating solar arrays? Research projects in which various densities, arrays, or designs of energy-development infrastructure are considered would be extremely valuable. BACI studies would be very useful for addressing this deficiency.

What are the best sites for energy farms with respect to the needs of wildlife? The large areas of public land available for renewable energy development in the desert Southwest encompass a wide variety of habitats. Although this provides a large number of choices for USSED, not all areas have the same energy potential because of resource availability and the limitations associated with engineering requirements, as was noted above. Detailed information on wildlife distribution and habitat requirements are crucially needed for proper site location and for the design of renewable energy developments (Tsoutsos et al. 2005). Public-resource-management agencies have access to rich geospatial data sets based on many years of inventories and resource-management planning. These data could be used to identify areas of high value for both energy development and wildlife. Areas with overlapping high values could be carefully studied through risk assessment when it appears that conflicts are likely. Previously degraded wildlife habitats, such as old mine sites, overgrazed pastures, and abandoned crop fields, may be good places to concentrate USSED to minimize its impacts on wildlife (CBI 2010).

Can the impacts of solar energy development on wildlife be mitigated? The construction of solar energy facilities can cause direct mortality of wildlife. In addition, building these facilities results in the destruction and fragmentation of wildlife habitat and may increase the possibility of fire, as was discussed above. Beyond these effects, essentially nothing is known about the operational effects of solar energy facilities on wildlife. Current mitigation strategies for desert tortoises and other protected species include few alternatives other than translocation of the animals from the footprint of the development into other areas. Although this strategy may be appealing at first glance, animal translocation has a checkered history of success, especially for reptiles and amphibians (Germano and Bishop 2008, CBI 2010). Translocation

has yet to be demonstrated as a viable long-term solution that would mitigate the destruction of Agassiz's desert tortoise habitat (Ernst and Lovich 2009, CBI 2010).

Conclusions

All energy production has associated social and environmental costs (Budnitz and Holdren 1976, Bezdek 1993). In their review of the adverse environmental effects of renewable energy development, Abbasi and Abbasi (2000) stated that "renewable energy sources are not the panacea they are popularly perceived to be; indeed, in some cases, their adverse environmental impacts can be as strongly negative as the impacts of conventional energy sources" (p. 121). Therefore, responsible, efficient energy production requires both the minimization of environmental costs and the maximization of benefits to society—factors that are not mutually exclusive. Stevens and colleagues (1991) and Martín-López and colleagues (2008) suggested that the analyses of costs and benefits should include both wildlife use and existence values. On the basis of our review of the existing peer-reviewed scientific literature, it appears that insufficient evidence is available to determine whether solar energy development, as it is envisioned for the desert Southwest, is compatible with wildlife conservation. This is especially true for threatened species such as Agassiz's desert tortoise. The many other unanswered questions that remain after reviewing the available evidence provide opportunities for future research, as was outlined above.

The shift toward renewable energy is widely perceived by the public as a "green movement" intended to reduce greenhouse-gas emissions and acid rain and to curb global climate change (Abbasi and Abbasi 2000). However, as was noted by Harte and Jassby (1978), just because an energy technology is simple, thermodynamically optimal, renewable, or inexpensive does not mean that it will be benign from an ecological perspective. The issue of wildlife impacts is much more complex than is widely appreciated, especially when the various scales of impact (e.g., local, regional, global) are considered. Our analysis shows that, on a local scale, so little is known about the effects USSEDO on wildlife that extrapolation to larger scales with any degree of confidence is currently limited by an inadequate amount of scientific data. Therefore, without additional research to fill the significant information void, accurate assessment of the potential impacts of solar energy development on wildlife is largely theoretical but needs to be empirical and well-founded on supporting science.

Acknowledgments

Earlier versions of the manuscript benefited from comments offered by Linda Gundersen, Marijke van Heeswijk, John Mathias, Misa Milliron, Ken Nussear, Mary Price, Mark Sogge, Linda Spiegel, and Brian Wooldridge. Special thanks to Emily Waldron and Caleb Loughran for their assistance with literature searches. The research was generously supported by a grant from the California Energy Commission, Research Development and Demonstration Division, Public Interest Energy Research program (contract # 500-09-020). Special thanks to Al Muth for providing accommodations at the Philip L. Boyd Deep Canyon Research Center of the University of California, Riverside, during the development of the manuscript. Any use of trade, product, or firm names is for descriptive purposes only and does not imply endorsement by the US government.

References cited

Abbasi SA, Abbasi N. 2000. The likely adverse environmental impacts of renewable energy sources. Applied Energy 65: 121–144.

Balmori A. 2010. The incidence of electromagnetic pollution on wild mammals: A new "poison" with a slow effect on nature? Environmentalist 30: 90–97.

Barber JR, Crooks KR, Fristrup KM. 2009. The costs of chronic noise exposure for terrestrial organisms. Trends in Ecology and Evolution 25: 180–189.

Bezdek RH. 1993. The environmental, health, and safety implications of solar energy in central station power production. Energy 18: 681–685.

Brattstrom BH, Bondello MC. 1983. Effects of off-road vehicle noise on desert vertebrates. Pages 167–206 in Webb RH, Wilshire HG, eds. Environmental Effects of Off-road Vehicles: Impacts and Management in Arid Regions. Springer.

Brooks ML, Esque TC. 2002. Alien plants and fire in desert tortoise (*Gopherus agassizii*) habitat of the Mojave and Colorado Deserts. Chelonian Conservation and Biology 4: 330–340.

Brooks ML, Matchett JR. 2006. Spatial and temporal patterns of wildfires in the Mojave Desert, 1980–2004. Journal of Arid Environments 67: 148–164.

Brown DE, Minnich RA. 1986. Fire and changes in creosote bush scrub of the western Sonoran Desert, California. American Midland Naturalist 116: 411–422.

Budnitz RJ, Holdren JP. 1976. Social and environmental costs of energy systems. Annual Review of Energy 1: 553–580.

[CBI] Conservation Biology Institute. 2010. Recommendations of Independent Science Advisors for the California Desert Renewable Energy Conservation Plan (DRECP). CBI. (6 July 2011; *www.energy.ca.gov/2010publications/DRECP-1000-2010-008/DRECP-1000-2010-008-F.PDF*)

Cowles RB. 1941. Observations on the winter activities of desert reptiles. Ecology 22: 125–140.

Delaney KS, Riley SPD, Fisher RN. 2010. A rapid, strong, and convergent genetic response to urban habitat fragmentation in four divergent and widespread vertebrates. PLoS ONE 5: e12767. doi:10.1371/journal.pone.0012767

Drewitt AL, Langston RHW. 2006. Assessing the impacts of wind farms on birds. Ibis 148: 29–42.

[EPRI] Electric Power Research Institute. 2002. Comparison of alternate cooling technologies for California power plants: economic, environmental, and other tradeoffs. California Energy Commission. Report no. 500–02–079F.

Ernst CH, Lovich JE. 2009. Turtles of the United States and Canada, 2nd ed. Johns Hopkins University Press.

Esque TC, Schwalbe CR, DeFalco LA, Duncan RB, Hughes TJ. 2003. Effects of desert wildfires on desert tortoise (*Gopherus agassizii*) and other small vertebrates. Southwestern Naturalist 48: 103–111.

Field JP, Belnap J, Breshears DD, Neff JC, Okin GS, Whicker JJ, Painter TH, Ravi S, Reheis MC, Reynolds RL. 2010. The ecology of dust. Frontiers in Ecology and the Environment 8: 423–430.

Flather CH, Knowles MS, Kendall IA. 1998. Threatened and endangered species geography. BioScience 48: 365–376.

Forman RTT, Alexander LE. 1998. Roads and their major ecological effects. Annual Review of Ecology and Systematics 29: 207–231.

Gee D. 2009. Late lessons from early warnings: Towards realism and precaution with EMF. Pathophysiology 16: 217–231.

Germano JM, Bishop PJ. 2008. Suitability of amphibians and reptiles for translocation. Conservation Biology 23: 7–15.

Gill AB. 2005. Offshore renewable energy: ecological implications of generating electricity in the coastal zone. Journal of Applied Ecology 42: 605–615.

Goodrich BA, Koski RD, Jacobi WR. 2008. Roadside vegetation health condition and magnesium chloride ($MgCl_2$) dust suppressant use in two Colorado, U.S. counties. Arboriculture and Urban Forestry 34: 252–259.

Harte J, Jassby A. 1978. Energy technologies and natural environments: The search for compatibility. Annual Review of Energy 3: 101–146.

Herbst DB. 2006. Salinity controls on trophic interactions among invertebrates and algae of solar evaporation ponds in the Mojave Desert and relation to shorebird foraging and selenium risk. Wetlands 26: 475–485.

Horváth G, Varjú D. 2004. Polarized Light in Animal Vision: Polarization Pattern in Nature. Springer.

Horváth G, Kriska G, Malik P, Robertson B. 2009. Polarized light pollution: A new kind of ecological photopollution. Frontiers in Ecology and the Environment 7: 317–325.

Hulin V, Delmas V, Girondot M, Godrey MH, Guillon JM. 2009. Temperature-dependent sex determination and global change: Are some species at greater risk? Oecologia 160: 493–506.

Khalil I, Sahm A, Boehm R. 2006. Wet or dry cooling? Pages 55–62 in Proceedings of ISEC 2006: International Solar Energy Conference; July 18–13, 2006, Denver, Co. Paper no. ISEC 2006-99082. doi:10.1115/ISEC2006-99082

Kristan WB III, Boarman WI. 2007. Effects of anthropogenic developments on common raven nesting biology in the west Mojave Desert. Ecological Applications 17: 1703–1713.

Kunz TH, Arnett EB, Erickson WP, Hoar AR, Johnson GD, Larkin RP, Strickland MD, Thresher RW, Tuttle MD. 2007. Ecological impacts of wind energy development on bats: Questions, research needs, and hypotheses. Frontiers in Ecology and the Environment 5: 315–324.

Kuvlesky WP Jr, Brennan LA, Morrison ML, Boydston KK, Ballard BM, Bryant FC. 2007. Wind energy development and wildlife conservation: Challenges and opportunities. Journal Wildlife Management 71: 2487–2498.

Lightfoot DC, Whitford WG. 1991. Productivity of creosotebush foliage and associated canopy arthropods along a desert roadside. American Midland Naturalist 125: 310–322.

Longcore T, Rich C. 2004. Ecological light pollution. Frontiers in Ecology and the Environment 2: 191–198.

Lovich JE, Bainbridge D. 1999. Anthropogenic degradation of the southern California desert ecosystem and prospects for natural recovery and restoration. Environmental Management 24: 309–326.

Lovich JE, Daniels R. 2000. Environmental characteristics of desert tortoise (*Gopherus agassizii*) burrow locations in an altered industrial landscape. Chelonian Conservation and Biology 3: 714–721.

Martín-López B, Montes C, Benayas J. 2008. Economic valuation of biodiversity conservation: The meaning of numbers. Conservation Biology 22: 624–635.

McCrary MD, McKernan RL, Schreiber RW, Wagner WD, Sciarrotta TC. 1986. Avian mortality at a solar energy power plant. Journal of Field Ornithology 57: 135–141.

Mittermeier R, Mittermeier CG, Robles Gil P, Fonseca G, Brooks T, Pilgrim J, Konstant WR, eds. 2002. Wilderness: Earth's Last Wild Places. Conservation International.

Munson SM, Belnap J, Okin GS. 2011. Responses of wind erosion to climate-induced vegetation changes on the Colorado Plateau. Proceedings of the National Academy of Sciences 108: 3854–3859.

Murphy RW, Berry KH, Edwards T, Leviton AE, Lathrop A, Riedle JD. 2011. The dazed and confused identity of Agassiz's land tortoise, *Gopherus agassizii* (Testudines, Testudinidae) with the description of a new species, and its consequences for conservation. ZooKeys 113: 39–71.

[NREL] National Renewable Energy Laboratory. 2011. Dynamic maps, GIS data and analysis tools: Solar maps. NREL. (6 July 2011; *www.nrel.gov/gis/solar.html*)

Pater LL, Grubb TG, Delaney DK. 2009. Recommendations for improved assessment of noise impacts on wildlife. Journal of Wildlife Management 73: 788–795.

Pearson DC. 1986. The desert tortoise and energy development in southeastern California. Herpetologica 42: 58–59.

Perry A, Bauer GB, Dizon AE. 1985. Magnetoreception and biomineralization of magnetite in amphibians and reptiles. Pages 439–453 in Kirschvink JL, Jones DS, MacFarland BJ, eds. Magnetite Biomineralization and Magnetoreception in Organisms: A New Biomagnetism. Plenum Press.

Perry G, Buchanan BW, Fisher RN, Salmon M, Wise SE. 2008. Effects of artificial night lighting on reptiles and amphibians in urban environments. Pages 239–256 in Jung RE, Mitchell JC, eds. Urban Herpetology. Society for the Study of Amphibians and Reptiles.

Petersen JK, Malm T. 2006. Offshore windmill farms: Threats to or possibilities for the marine environment. Ambio 35: 75–80.

Piechota T, van Ee J, Batista J, Stave K, James D, eds. 2004. Potential and environmental impacts of dust suppressants: "Avoiding another Times Beach." US Environmental Protection Agency. Panel Summary no. EPA/600/R-04/031. (6 July 2011; *www.epa.gov/esd/cmb/pdf/dust.pdf*)

Pimentel D, et al. 1994. Renewable energy: economic and environmental issues. BioScience 44: 536–547.

Randall JM, Parker SS, Moore J, Cohen B, Crane L, Christian B, Cameron D, MacKenzie JB, Klausmeyer K, Morrison S. 2010. Mojave Desert Ecoregional Assessment. The Nature Conservancy. (6 July 2011; *http://conserveonline.org/workspaces/mojave/documents/mojave-desert-ecoregional-2010/@@view.html*)

Sawyer H, Kauffman MJ, Nelson RM. 2009. Influence of well pad activity on winter habitat selection patterns on mule deer. Journal of Wildlife Management 73: 1052–1061.

Schlesinger WH, Fonteyn PJ, Reiner WA. 1989. Effects of overland flow on plant water relations, erosion, and soil water percolation on a Mojave Desert landscape. Soil Science Society of America Journal 53: 1567–1572.

Sharifi MR, Gibson AC, Rundel PW. 1997. Surface dust impacts on gas exchange in Mojave Desert shrubs. Journal of Applied Ecology 34: 837–846.

Sharma VP, Kumar NR. 2010. Changes in honeybee behaviour and biology under the influence of cellphone radiations. Current Science 98: 1376–1378.

Singh V, Piechota TC, James D. 2003. Hydrologic impacts of disturbed lands treated with dust suppressants. Journal of Hydrologic Engineering 8: 278–286.

Stebbins RC. 1995. Off-road vehicle impacts on desert plants and animals. Pages 467–480 in Latting J, Rowlands PG, eds. The California Desert: An Introduction to Natural Resources and Man's Impact, vol. 2. June Latting Books.

Stevens TH, Echeverria J, Glass RJ, Hager T, More TA. 1991. Measuring the existence value of wildlife: What do CVM estimates really show. Land Economics 67: 390–400.

Suter AH. 2002. Construction noise: Exposure, effects, and the potential for remediation; a review and analysis. American Industrial Hygiene Association Journal 63: 768–789.

Torcellini P, Long N, Judkoff R. 2003. Consumptive Water Use for U.S. Power Production. National Renewable Energy Laboratory. Report no. NREL/TP-550-33905.

Tracy CR, Brussard PF. 1994. Preserving biodiversity: Species in landscapes. Ecological Applications 4: 205–207.

Tsoutsos T, Frantzeskaki N, Gekas V. 2005. Environmental impacts from solar energy technologies. Energy Policy 33: 289–296.

[USDOI and USDOE] US Department of the Interior, US Department of Energy. 2011a. Draft Programmatic Environmental Impact Statement for Solar Energy Development in Six Southwestern States. US Department of Energy. Report no. DOE/EIS-0403. (19 September 2011; *http://solareis.anl.gov/documents/dpeis/index.cfm*)

———. 2011b. Supplement to the Draft Programmatic Environmental Impact Statement for Solar Energy Development in Six Southwestern States. (2 November 2011; *http://solareis.anl.gov/news/index.cfm*)

———. 2011c. Notice of availability of the supplement to the draft programmatic environmental impact statement for solar energy development in six southwestern states and notice of public meetings. Federal Register 76: 66958–66960.

[USEPA] US Environmental Protection Agency. 2010. National Environmental Policy Act. USEPA. (5 July 2011; *www.epa.gov/oecaerth/basics/nepa.html#oversight*)

Von Seckendorff Hoff K, Marlow RW. 2002. Impacts of vehicle road traffic on desert tortoise populations with consideration of conservation of tortoise habitat in southern Nevada. Chelonian Conservation and Biology 4: 449–456.

Webb RH. 1983. Compaction of desert soils by off-road vehicles. Pages 51–79 in Webb RH, Wilshire HG, eds. Environmental Effects of Off-road Vehicles: Impacts and Management in Arid Regions. Springer.

Webb RH, Fenstermaker LF, Heaton JS, Hughson DL, McDonald EV, Miller DM, eds. 2009. The Mojave Desert: Ecosystem Processes and Sustainability. University of Nevada Press.

White PJ, Broadley MR. 2001. Chloride in soils and its uptake and movement within the plant: A review. Annals of Botany 88: 967–988.

Wilshire HG, Nielson JE, Hazlett RW. 2008. The American West at Risk: Science, Myths, and Politics of Land Abuse and Recovery. Oxford University Press.

Jeffrey E. Lovich (jeffrey_lovich@usgs.gov) is a research ecologist, and Joshua R. Ennen (josh.ennen@maryvillecollege.edu) was a wildlife biologist, both with the US Geological Survey, Southwest Biological Science Center. Ennen is now with Maryville College in Tennessee. The authors are studying the effects of utility-scale renewable energy development on terrestrial vertebrates, especially Agassiz's desert tortoise.

EXHIBIT 9

Large endolymphatic potentials from low-frequency and infrasonic tones in the guinea pig

Alec N. Salt,[a] Jeffery T. Lichtenhan, Ruth M. Gill, and Jared J. Hartsock
Department of Otolaryngology, Washington University School of Medicine, St. Louis, Missouri 63110

(Received 1 August 2012; revised 12 December 2012; accepted 9 January 2013)

Responses of the ear to low-frequency and infrasonic sounds have not been extensively studied. Understanding how the ear responds to low frequencies is increasingly important as environmental infrasounds are becoming more pervasive from sources such as wind turbines. This study shows endolymphatic potentials in the third cochlear turn from acoustic infrasound (5 Hz) are larger than from tones in the audible range (e.g., 50 and 500 Hz), in some cases with peak-to-peak amplitude greater than 20 mV. These large potentials were suppressed by higher-frequency tones and were rapidly abolished by perilymphatic injection of KCl at the cochlear apex, demonstrating their third-turn origins. Endolymphatic iso-potentials from 5 to 500 Hz were enhanced relative to perilymphatic potentials as frequency was lowered. Probe and infrasonic bias tones were used to study the origin of the enhanced potentials. Potentials were best explained as a saturating response summed with a sinusoidal voltage (V_o), that was phase delayed by an average of 60° relative to the biasing effects of the infrasound. V_o is thought to arise indirectly from hair cell activity, such as from strial potential changes caused by sustained current changes through the hair cells in each half cycle of the infrasound. © *2013 Acoustical Society of America*.
[http://dx.doi.org/10.1121/1.4789005]

PACS number(s): 43.64.Nf [CAS] Pages: 1561–1571

I. INTRODUCTION

The ear possesses numerous mechanisms to reduce the sensitivity to low-frequency sounds. Mechanically, the middle ear attenuates low-frequency sounds by ~6 dB/octave as frequency is lowered below 1 kHz (Dallos, 1973; Cheatham and Dallos, 2001). The helicotrema shunts pressure between scala tympani (ST) and scala vestibuli, attenuating low-frequency stimulation by ~6 dB/octave below 100 Hz both in humans (Dallos, 1970) and in guinea pigs (Franke and Dancer, 1982; Salt and Hullar, 2010). The stereocilia of the inner hair cells (IHCs) are not directly coupled to the tectorial membrane but are stimulated by fluid movements in the subtectorial space (Nowotny and Gummer, 2006; Guinan, 2012); this causes IHCs to be sensitive to basilar membrane velocity and attenuates low-frequency input by 6 dB/octave below ~470 Hz (Cheatham and Dallos, 2001). As hearing is mediated by IHCs, these mechanisms combine to make hearing very insensitive to low-frequency sounds and infrasound. As an example, a 5 Hz tone must be presented at ~109 dB SPL for humans to hear it (Møller and Pederson, 2004).

The studies reported here were performed with guinea pigs, a species for which the perception of infrasonic frequencies has never been measured. The ability to detect low frequencies has been correlated with cochlear length for species such as humans and guinea pigs with results showing that shorter cochleae are typically less sensitive to low frequencies (West, 1985; Echteler *et al.*, 1994). As compared to humans, guinea pigs require an average of 15 dB higher sound pressure level over the low-frequency range that has been measured (50–500 Hz; Heffner *et al.*, 1971; Miller and Murray, 1966; Prosen *et al.*, 1978; Walloch and Taylor-Spikes, 1976). We therefore expect guinea pigs to be less sensitive to infrasonic stimulation than humans and estimate the perceptual threshold for 5 Hz to be ~124 dB SPL. Thus responses to infrasonic frequencies are expected to be more robust in human cochleae than in guinea pigs.

In contrast to the IHCs, which are fluid coupled to the mechanical input, the stereocilia of the outer hair cells (OHCs) are directly coupled to the tectorial membrane, thus making OHCs sensitive to organ of Corti displacement (Dallos *et al.*, 1982; Dallos, 1986). Early studies by von Békésy (1951, 1960) showed that when the organ of Corti was displaced in a sustained manner by a mechanical probe, such as with a trapezoidal stimulus, the voltage response was sustained for the duration of the stimulus. These classic studies demonstrated that OHCs are capable of responding to very low frequencies. Salt and DeMott (1999) applied low-frequency stimulation by fluid injections into the perilymph and showed that large potentials, over 20 mV peak to peak (pk/pk) in amplitude, were generated in the endolymphatic space at stimulus frequencies from 10 Hz down to 0.1 Hz. Although stimulus delivery in this study was not by a normal, physiological route, responses of comparable magnitude were found during spontaneous middle-ear muscle contractions; this demonstrated that large potentials can indeed be elicited by physiologic stimuli. The amplitude of the cochlear microphonics (CMs) from stimuli in the range of audibility are typically less than ~2–3 mV pk/pk when measured in perilymph but have been shown to be up to ~8 mV pk/pk when recorded from the endolymph space of the apical cochlear turns (Honrubia and Ward, 1968; Honrubia *et al.*, 1973; Dallos, 1973). Salt *et al.* (2009) showed that

[a]Author to whom correspondence should be addressed. Electronic mail: salta@ent.wustl.edu

increases of endocochlear potential (EP) by more than 10 mV occurred when the organ of Corti was displaced toward scala tympani for a period of minutes by the slow injection of gel into the cochlear apex. These studies suggest that when the organ of Corti is displaced by low-frequency sounds, CM changes associated with OHC stimulation are greatest when recorded from the endolymphatic space.

In the present report, we examine the cochlear responses elicited by infrasonic and low-frequency acoustic stimulation. The issue of sensitivity to low-frequency sounds is becoming of greater importance because low-frequency environmental sounds are becoming more pervasive. People with wind turbines located near their homes can be exposed to low-frequency stimulation for prolonged periods of time (Jakobsen, 2005; van den Berg, 2006; O'Neal *et al*., 2011; Møller and Pedersen, 2011). Because infrasound is not heard, it is commonplace to high-pass filter the measured sounds with cutoff frequencies derived from the human audibility curve (A-weight) thereby diminishing low-frequency components (e.g., Møller and Pedersen, 2011). Other weighting functions give greater emphasis to infrasonic frequencies, such as G-weighting, which filters below 1 Hz and above 20 Hz at 24 dB/octave and emphasizes frequencies between 1 and 20 Hz according to their perceptual audibility (Broner, 2008). Wind turbines of contemporary design typically generate infrasonic levels of $\leq$70 dB G that are well below the 90 dB G level required for subjective hearing (Jakobsen, 2005; ISO, 1996). As infrasound levels from wind turbines are typically below the threshold of hearing, it has been widely concluded that the low-frequency components of the sound can be ignored. This has been encapsulated by the widely used quotation "What you can't hear, won't hurt you," which was attributed to an engineer named Campanella by Alves-Pereira and Castelo Branco (2007). Found elsewhere are numerous additional reports of wind-turbine noise assessments concluding that the infrasound level is insignificant because it is not heard (e.g., O'Neal *et al*., 2011). This particular subgenre of noise measurement and regulation is therefore almost entirely based on human *perception*. Our objective measures, such as those reported here, lead us to strongly advocate that before effects on humans can be dismissed, we must better understand the nature of the ear's response to infrasound in much greater detail.

II. METHODS

A. Animal preparation

This study used 13 guinea pigs under animal protocols 20070147 and 20100135 approved by the Animal Studies Committee of Washington University. Guinea pigs were initially anesthetized with 100 mg/kg sodium thiobutabarbital and maintained on 0.8%–1.2% isofluorane in oxygen. The trachea was cannulated, and the animal was artificially ventilated. End-tidal CO_2 was monitored with a capnograph (CapnoTrueAMP, Zevenaar, The Netherlands), and the tidal volume of the ventilator was adjusted to maintain an end-tidal CO_2 level of 5%. Body temperature was maintained at 38.5 °C with a DC-powered thermistor controlled heating pad. Pavulon (muscle relaxant) was given intravenously to suppress middle ear muscle contractions. The auditory bulla was exposed by a ventral approach and opened for the placement of recording electrodes.

B. Stimulus generation and delivery

Acoustic stimuli were delivered in a closed sound system. The external canal was sectioned and a hollow ear bar was inserted. An Etymotic Research ER-10 C acoustic assembly terminated near the tip of the earbar that also incorporated a Sennheiser HD 580 driver mounted in an acrylic coupler used to deliver low-frequency sounds. A probe tube to connect to a B&K 4134, [1/4]-in. reference microphone was also routed to the earbar. The B&K microphone was used to verify low-frequency calibrations, as it had a flat frequency response while the ER10C microphone incorporated low-frequency filtering.

Stimulus generation and data collection were performed with Tucker Davis System 3 hardware, driven by a custom written program (Microsoft Visual Basic) with ActiveX drivers. Three output channels were utilized, each routed though a Tucker Davis PA5 attenuator and Tucker Davis HB7 headphone amplifier. Sounds were calibrated in [1/4] octave steps from 4 Hz to 8 kHz for the Sennheiser transducer and 125 Hz to 22 kHz for the ER10C drivers.

C. Recording procedures

Most of the cochlear responses reported here were recorded through glass microelectrodes beveled to 4–6 μm tip outer diameter and filled with 500 mM KCl or 500 mM NaCl for endolymphatic and perilymphatic recordings, respectively. Electrodes were connected through Ag/AgCl wires and high input impedance ($>10^{14}$ Ω) DC-coupled amplifiers to the data acquisition system. The reference electrode was an Ag/AgCl pellet [RC1, World Precision Instruments (WPI), Sarasota, FL] connected though a fluid bridge to the muscles of the neck. In most cases, responses from endolymph and perilymph in the same cochlear turn were recorded simultaneously. Some responses (e.g., CAPs to high-frequency stimuli) were also recorded from an Ag/AgCl ball electrode placed on the edge of the round-window membrane near the bony annulus that was routed to a Tucker-Davis DB4 amplifier with the high-pass filter set at 5 Hz.

Four input channels of the Tucker-Davis system were sampled simultaneously, typically representing signals from the round window electrode, the ear canal microphone and two dc-coupled inputs from electrometers. An automated CAP audiogram was initially performed (1–22 kHz in [1/4] octave steps) to verify normal cochlear function. Measuring responses to low stimulus frequencies required collection windows of 4–6 s duration—a time consuming process when multiple response are averaged. Collection windows were therefore varied when measuring responses to stimuli of different frequency. For potential amplitude measurement algorithms, windows of 2 s, 200 ms, and 20 ms were used for frequencies below 25 Hz, from 25 to 250 Hz, and above 250 Hz, respectively. In most cases, dc-coupled responses were recorded. When responses to low-level stimuli were recorded for isopotential curves, band-pass filtering centered at the stimulus

frequency was used to reduce noise. At each frequency, a response average with no stimulus was performed to verify that the background noise was less than 60% of the criterion response amplitude of 100 μV.

D. Cochlear fluids manipulations

The sites of origin of cochlear responses were evaluated using an injection of isotonic KCl into perilymph at the apex to ablate sensory function progressively from apex to base. KCl solution was injected from a glass pipette coupled to a gas-tight syringe mounted on a digitally controlled pump (Ultrapump, WPI, Sarasota, FL). The pipette was sealed into the apex using established procedures that are documented elsewhere (Salt *et al.*, 2009). The mucosa covering the cochlear bone was removed at the apex, the bone was dried, and a thin layer of cyanoacrylate glue was applied that was covered with a thin layer of two-part silicone (Kwik-Cast, WPI, Sarasota, FL) to create a hydrophobic surface. A ~50 μm diameter fenestration was made through the adhesives and bone at the cochlear apex, and the tip of the injection pipette was inserted into perilymph. A tissue wick was used to remove the fluid droplet accumulating at the perforation site, and a drop of cyanoacrylate was immediately applied to seal the fenestration. Injection from a pipette sealed into the cochlea causes fluid flow to be directed toward the cochlear aqueduct at the basal turn of ST, displacing perilymph through the aqueduct into the ventricles. This results in an apical-to-basal progression of KCl that progressively ablates sensory cell function. Because the cross-sectional area of ST increases from apex to base, a constant injection rate would have caused the KCl front to slow as it approached the basal turn. We therefore progressively increased flow rate, from 50 nl/min (0–10 min), 100 nl/min (10–30 min), and 200 nl/min (≥30 min). The movement of KCl along the cochlea with this injection protocol was calculated using our established model of the cochlear fluids (available at http://oto.wustl.edu/cochlea/), which takes into account scala dimensions with distance, diffusion, flow rate, and communications with adjacent compartments.

E. Cochlear microphonic waveform analysis

To interpret CM response waveforms measured from endolymph, an analysis was performed in which the saturating response of the cochlear transducer was represented by a Boltzmann function driven by input sinusoids corresponding to the probe and bias stimuli. This approach is comparable to prior studies (Patuzzi and Moleirinho, 1998; Sirjani *et al.*, 2004; Brown *et al.*, 2009). The Boltzmann function used was similar to that described by Brown *et al.* (2009):

$$V_t = V_{EP} + (-V_{sat} + 2 \cdot V_{sat}/ (1 + \exp(-2 \cdot S_B/V_{sat}(P_t)))), \quad (1)$$

where V_{EP} is a DC potential representing the endocochlear potential magnitude (mV), V_{sat} is the saturation voltage of the Boltzmann curve (mV), S_B represents the slope of the Boltzmann curve at its mid-point (mV/Pa), P_t represents the input pressure (Pa) as a function of time.

Input to the function (P_t) was calculated as the sum of three independent inputs

$$P_t = P_{probe,t} + P_{bias,t} + OP,$$

where $P_{probe,t} = A_{probe} * \sin(2\pi f_{probe} t + \Phi_{probe})$ represents the probe tone (Pa) and $P_{bias,t} = A_{bias}/S * \sin(2\pi f_{bias} t + \Phi_{bias})$ represents the bias tone. OP represents the operating point of the transducer (Pa), defined as the pressure (i.e., the location on the Boltzmann curve) when probe and bias pressures are both zero. The variables A, f, and Φ define the amplitude, frequency and phase of the input tones respectively. S is a scale factor used to compensate for the difference in sensitivity to probe and bias tones at the specified sound pressure levels.

For some conditions, an additional sinusoidal potential at the frequency of the bias tone (f_{bias})was summed with the Boltzmann output as shown in Eq. (2).

$$V_t = V_{EP} + (-V_{sat} + 2 \cdot V_{sat}/ (1 + \exp(-2 \cdot S_B/V_{sat}(P_t)))) + V_o \cdot \sin(2\pi f_{bias} t + \Phi_{bias} + \Phi_o), \quad (2)$$

where V_o defines amplitude and Φ_o defines the phase of the potential relative to that of the bias tone Φ_{bias}. Calculated waveforms from Eqs. (1) and (2) were fitted to measured CM waveforms (5086 points) using the Solver add-in of Microsoft EXCEL. Best fit was established by minimizing the sum of squares of differences between measured and calculated waveforms.

III. RESULTS

A. Response amplitudes

Figure 1 shows an example recording from endolymph of the third turn of a guinea pig cochlea using a 5 Hz stimulus presented at 120 dB SPL. The pk/pk response amplitude was 19.1 mV—a sizable (23%) modulation of the resting EP that was 83.1 mV in this animal. The large amplitude of responses poses a scientific conundrum as 5 Hz presented at this level should be close to the subjective threshold, which we estimated earlier in Sec. I to be approximately 124 dB SPL in guinea pigs.

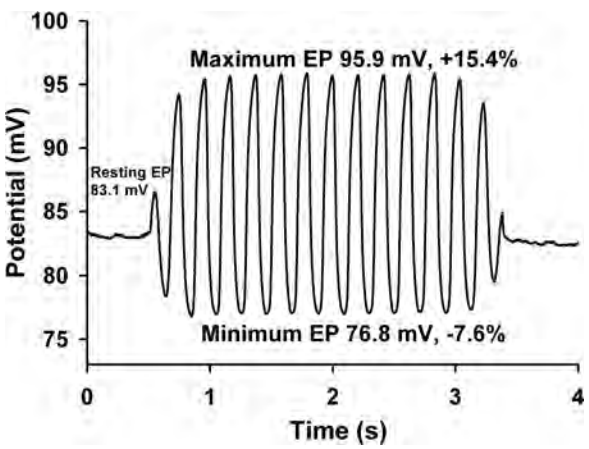

FIG. 1. Measured endolymphatic potential from cochlear turn 3 during stimulation with a single 5 Hz tone burst at 120 dB SPL. The sinusoidal potential represents a modulation of the normal (83.1 mV) endocochlear potential by over 20%.

CM response amplitudes (input/output functions) to low-frequency stimuli (5, 50, and 500 Hz) measured at four cochlear locations are summarized in Fig. 2. At each location, CM amplitudes exhibit the classic linear response with lower level stimuli and saturation with high level stimuli. In endolymph of turn 3 [Fig. 2(A)], although the response to 5 Hz at low levels (60 dB SPL, for example) was smaller than that to 50 or 500 Hz, the responses to 5 Hz at high levels did not saturate to the same degree as the higher frequencies such that the 5 Hz response was substantially larger (as indicated by the arrow). At the highest stimulus level tested (115 dB SPL) the peak amplitudes in endolymph of the third turn averaged 17.1 mV, and the largest individual responses were above 20 mV. These large responses to infrasound appear to be an apical endolymphatic phenomenon. Responses to 5 Hz were lower both in basal first turn endolymph [Fig. 2(B)] and in third turn perilymph [Fig. 2(C)]. Responses to 5 Hz were extremely small in first turn perilymph [Fig. 2(D)] and would likely be not detectable by conventional recordings from the round window membrane. The response amplitudes for infrasonic (5 Hz) stimuli in endolymph of the third turn were substantially larger than the maximum generated by tones in the normal range of audibility presented at any level.

The relative sensitivity across frequency from 5 to 1000 Hz measured as isoamplitude functions is shown in Fig. 3. In perilymph of the first and third cochlear turns, sensitivity decreased as frequency was lowered by approximately 7 and 10 dB/octave, respectively, from 500 to 50 Hz and 6 dB/octave for both turns between 50 and 5 Hz. In endolymph, the decline of sensitivity as frequency was lowered was less with slopes near 5 dB/octave from 500 to 5 Hz. The difference in sensitivity between endolymph and perilymph in each turn is shown in the lower panel of Fig. 3. The difference is in the 10–15 dB range around 500 Hz but increases progressively as frequency is lowered, so that endolymph measurements are 20–25 dB more sensitive than perilymph measurements in the 5–50 Hz range. This further demonstrates that responses measured from endolymph of the third turn to very low frequencies are far more sensitive than measured at other cochlear locations.

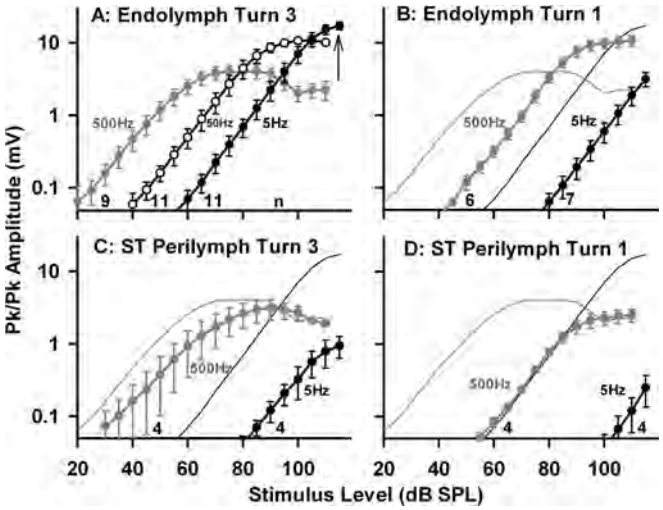

FIG. 2. Cochlear microphonic response amplitudes for 500 Hz (gray symbols), 50 Hz (open symbols), and 5 Hz (black symbols) stimulation recorded from four cochlear locations. Bars indicate s.d. Data for 50 Hz are only shown on (A) for clarity but were always intermediate between 5 and 500 Hz. Data from turn 3 endolymph are shown as thin lines on (B) through (D) for comparison. Responses from endolymph of turn 3 to 5 Hz were less sensitive than to 500 Hz at low stimulus levels but did not saturate to the same degree and markedly exceeded 500 Hz responses at high levels [indicated by the arrow on (A)]. Responses to 5 Hz were substantially lower in basal turn endolymph (B) and in third turn perilymph (C) and were almost absent from basal turn perilymph (D). At high stimulus levels, third turn endolymphatic potentials from infrasound (5 Hz, solid black symbols) were larger than for higher-frequency sounds presented at any level.

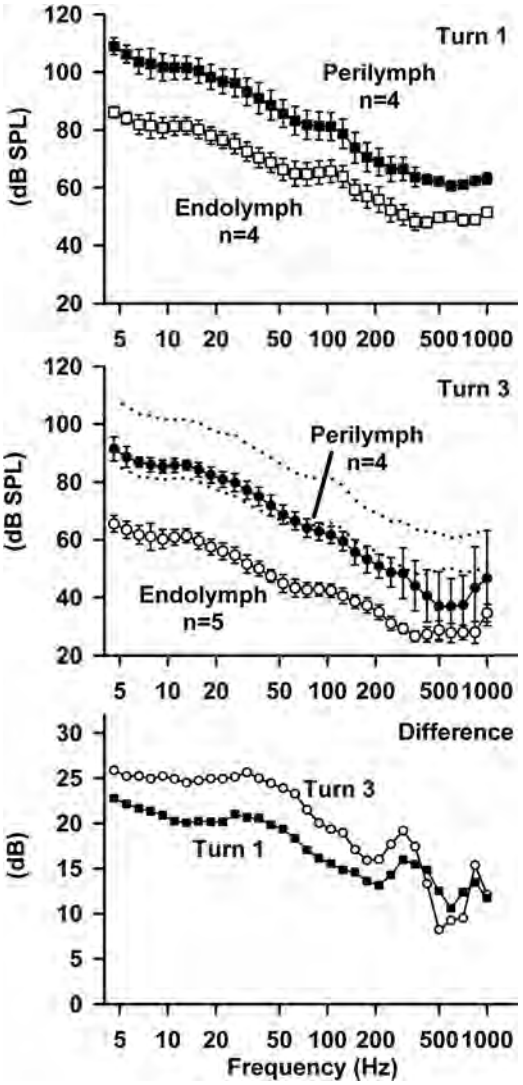

FIG. 3. Isopotential curves (100 μV) measured from 5 to 1000 Hz. Bars indicate s.d. Potentials were measured from endolymph (open symbols) and scala tympani perilymph (solid symbols) in cochlear turn 1 (top panel) and turn 3 (middle panel). At all probe-tone frequencies, a lower stimulus level was needed to evoke a 100 μV endolymphatic potential than for a perilymphatic potential. For comparison to cochlear turn 3 data, turn 1 data from the upper panel are shown as dotted lines in the middle panel (highest dotted line from perilymph and lowest dotted line from endolymph). Lower stimulus levels were needed to achieve a 100 μV turn 3 response in both scalae compared to turn 1. Turn 3 perilymph potentials from higher frequency probes were more variable due to higher background noise levels. The lower panel shows the mean endolymph-perilymph difference for the cochlear turns 1 and 3. The difference increased as frequency is lowered.

B. Origins of the large endolymphatic potentials

The origins of the large potentials recorded in endolymph were studied by injection of isotonic KCl from a pipette sealed into the cochlear apex. Injections into the sealed cochlea at rates 50 nl/min increasing to 200 nl/min result in a progressive apical to basal elevation of K^+ in ST; this ablates sensory cell function. The calculated K^+ concentration increases at different cochlear locations, based on the injection protocol used and guinea pig cochlear dimensions, are shown in the top panel of Fig. 4. The middle panel shows changes of EP and CM recorded from different locations, and the bottom panel shows CAP thresholds, each repeatedly measured through time during the injection in the same experiment. The CM to 4.8 and 238 Hz recorded from endolymph of turn 3 are the first responses to be affected by the injection. Around 17 min, the responses had both been reduced to less than 20% of the original amplitude—a decrease that occurred before CAP thresholds at any frequency had been affected. Responses recorded from the turn 1 electrode declined more slowly, consistent with their basal turn origins. CAP thresholds were progressively elevated in sequence from low to high frequencies, demonstrating the progressive and systematic dysfunction apex to base. EP magnitude from turns 1 and 3 declined more slowly than the sound-evoked potentials. These data, which were replicated in other experiments, demonstrate that the 5 Hz responses recorded from turn 3 endolymph have local origins in the apical regions of the cochlea.

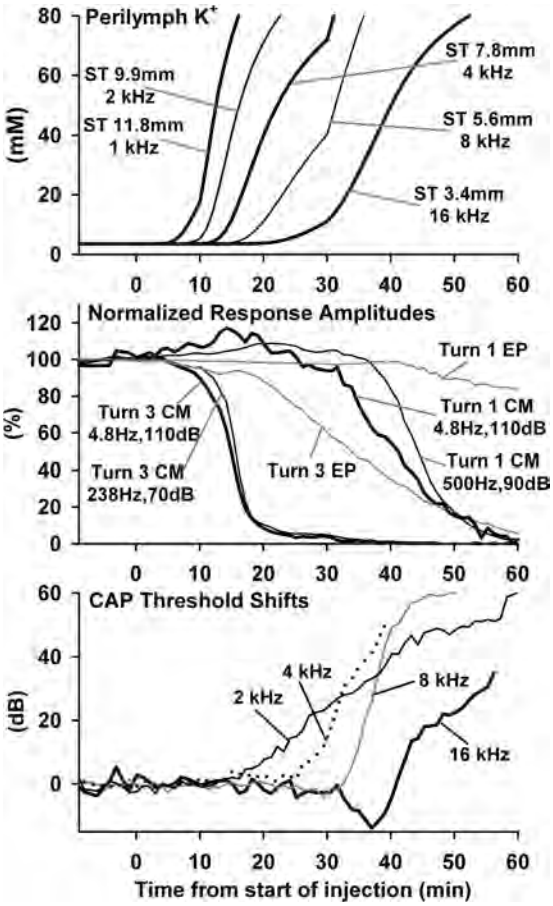

FIG. 4. Demonstration that third turn endolymphatic potentials are locally generated. Top: Calculated perilymph K^+ concentration increases at different locations along scala tympani (ST) resulting from the apical injection of KCl solution, starting at zero time. Labels indicate the distances along ST from the base in millimeters together with the best frequency of each location. The rate of injection increased with time so that the progression of KCl concentration increase occurred more uniformly even as the cross-sectional area of ST was increasing toward the base. Middle: Measured potentials from different cochlear locations repeated at 1 min intervals during the injection. All evoked potential measurements shown here were recorded in the same experiment. Responses from the third turn with 4.8 Hz, 110 dB SPL and 238 Hz, 70 dB SPL stimuli began decreasing after ~10 min while responses from turn 1 with 4.8 Hz, 110 dB SPL and 500 Hz, 90 dB SPL took much longer to decrease. The endocochlear potentials from the third and first turns declined more slowly than the sound induced responses. Bottom: Compound action potential (CAP) threshold shifts recorded at the round window at specific tone-burst frequencies as indicated. CAP thresholds increased sequentially from low to high frequencies as the KCl solution progressively moved down the cochlea with time. The 4.8 Hz response recorded from turn 3 (middle panel) was substantially reduced before the 2 kHz CAP—the lowest CAP tone-burst frequency—threshold was elevated, clearly showing that it was generated from an apical region.

C. Infrasound biasing studies

The existence of potentials generated locally in the third turn with amplitudes larger than the voltage at which CM saturates with higher frequency stimuli led us to consider how such large potentials could be generated by cochlear transduction. We studied this by combining a probe tone that saturated the transducer with an infrasonic bias tone that would normally generate responses of large amplitude. In previous biasing studies, the focus has typically been on how slow displacements of the sensory structures caused by bias tones influence responses to higher-frequency probe stimuli. The present study differs in that we wanted to understand the influence of probe tones on response to bias tones to study the origins in the infrasonic responses For this purpose, we needed a probe tone to partially saturate mechanoelectric transduction to define the transducer characteristics. However, probe tones at the required levels strongly suppressed the response to infrasonic bias tones. Figure 5 shows a paradigm in which a 500 Hz probe tone was superimposed on a 4.8 Hz infrasonic bias tone. As the level of the 500 Hz tone was increased, the response to 4.8 Hz was strongly suppressed. Suppression of bias responses has been reported elsewhere (Cheatham and Dallos, 1982, 1994). The response amplitude during the 4.8 Hz-alone segment (Infra Alone) was measured as the amplitude of a 4.8 Hz sinusoid that was best fit to the CM. The response amplitudes to both the probe and bias components when both were presented simultaneously were measured by fitting the sum of a 4.8 Hz sinusoid and a 500 Hz sinusoid passed through a Boltzmann function (representing the saturating response to the probe). This allowed both bias- and probe-response amplitudes to be independently quantified, as shown in the middle panel. It is apparent that the response to the infrasonic tone in the presence of the probe [Fig. 5(B) labeled "Infra + (probe)"] was suppressed at probe levels as low as 65 dB SPL, which is well below the 80–85 dB SPL where saturation of the probe occurs [Fig. 5(B) labeled "Probe + (infra)"]. However, the suppression was caused by the saturation associated with the response to the probe as shown in Figs. 5(C) and 5(D). In Fig. 5(C), the amplitude of the response to the probe was compared with a linear, theoretical

response in which response amplitude increases by 1 dB/dB. Deviations from this line became progressively greater as the probe level increased and responses became saturated. This shows that saturation starts occurring at probe levels well below those that produce maximum response amplitude. In Fig. 5(D), the response to infrasound was multiplied by the ratio of the probe response to the theoretical line, thus scaling the infrasound response to the same extent as the probe response saturates. The calculated curve [Fig. 5(D), dark solid line] closely matched the measured reduction of infrasound responses with increasing probe level, suggesting that physiological processes associated with saturation of the probe accounted for the suppression of the infrasound response.

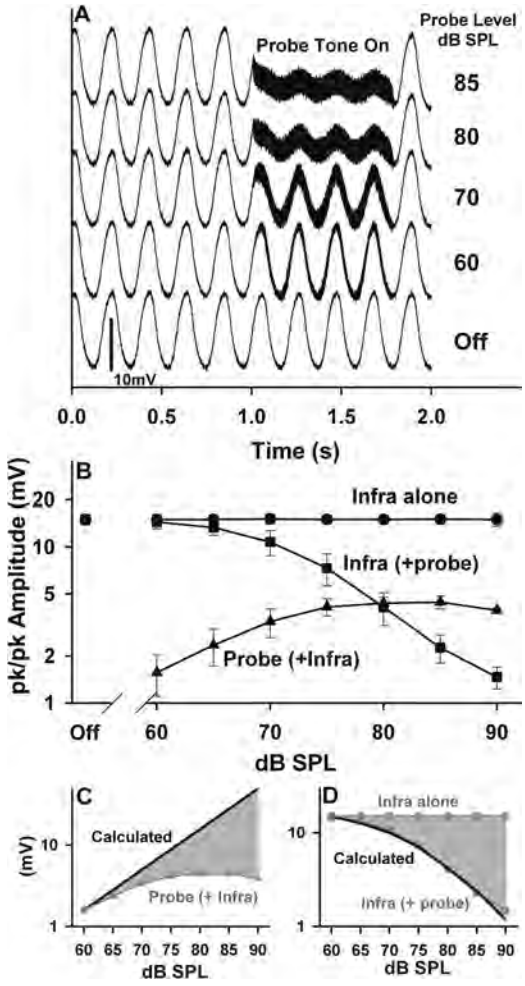

FIG. 5. (A) Influence of a 500 Hz probe tone added to an infrasonic (infra) stimulus (4.8 Hz, 110 dB SPL). Endolymphatic potentials were recorded from the third turn as a single epoch with no averaging. As the level of the probe tone increased, the response to infrasound was strongly suppressed. (B) Measured response amplitudes averaged in three animals. Bars indicate s.d. "Infra alone" indicates the amplitude of the infrasound response when presented alone. "Infra(+probe)" indicates the amplitude of the infrasound response when the probe was simultaneously on. "Probe(+infra)" indicates the amplitude of the probe response measured with the infrasound simultaneously on. (C) The measured response to the probe is compared with a linear (1 dB/dB) function. (D) The calculated curve shows the response to the infrasound tone alone corrected for the amplitude ratio of the probe relative to the calculated line from (C). The calculated curve closely fits the measured infrasound amplitude with the probe on. This demonstrates that the suppression of the infrasonic response arose from probe-tone-induced changes in the mechanoelectric transducer function.

An analysis of CM responses to infrasound in the presence of probe tones therefore needed to consider the suppression of the infrasound response by the probe at levels that even partially saturated the transducer. We were primarily interested in the origins of the large infrasound responses in the absence of a probe. Responses were therefore initially measured at a constant level of infrasound as the probe tone was varied in level. dc-coupled CM measurements from endolymph of the third turn with a fixed-level infrasonic bias tone (4.8 Hz, 110 dB SPL) and varied level of 238 Hz stimulation are illustrated in Fig. 6. Responses averaged to 10 bias-tone cycles are displayed as a single bias cycle. At low probe levels, the response to 238 Hz was highly modulated but as probe level was increased the degree of modulation decreased and the amplitude of the response to the 4.8 Hz bias tone was reduced. A notable feature in these recordings is that the regions where there was most saturation of the probe tone—indicated by asterisks on the 75 dB SPL trace—did not coincide with the times of minimum or maximal potential produced by the bias. This was a consistent finding in all animals tested. This means that the greatest influence of biasing on the probe response did not coincide in time with the largest bias-induced endolymphatic potentials.

A theoretical calculation showing the output from a saturating transducer represented by a first-order Boltzmann curve [Eq. (1)] in response to combined probe-plus-bias input stimuli is shown in Fig. 7. An asymmetry between the calculated output during negative and positive bias half-cycles, as seen in the experimental data, was produced by setting the operating point to a non-zero value [indicated by the black circle on Fig. 7(B)]. The operating point represents the resting position on the curve with no stimulus present. With a Boltzmann function of this type, the maximum and minimum voltages to

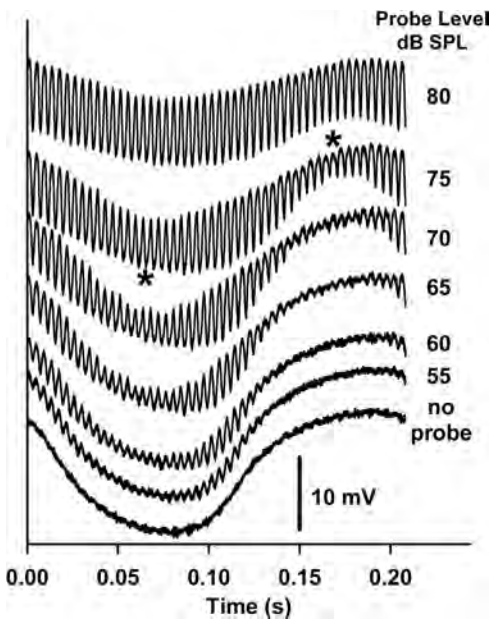

FIG. 6. Responses measured from the endolymphatic space of the third turn with a 4.8 Hz bias tone at 110 dB SPL and a 238 Hz probe tone that was varied in level. Responses are shown for a single cycle of the bias tone. As the probe level increased, the degree of modulation of the probe and the response amplitude to the bias both decreased. Additionally, the time when there was maximum saturation of the probe-tone response (asterisks) did not coincide with the times of maximum or minimum voltage generated by the bias.

the bias tone occur when the probe response is displaced at extremes of the curve and cause maximum saturation of the probe response. Single probe-tone cycles at extreme displacements are shown as dark thin lines on Fig. 7(C). This analysis did not provide a good representation of the measured responses from endolymph.

A solution that better represented the measured data was provided by a modification of the analysis in which a separate bias-generated sinusoidal potential was summed with the Boltzmann output, as represented in Eq. (2). This approach was initially justified by prior observations that tone-induced responses in endolymph could be offset by many millivolts during gel injections into the cochlear apex causing sustained displacements of the organ of Corti (Salt *et al*., 2009). Adding a phase-delayed potential at the bias frequency to the model allowed it to closely fit the measured CM waveforms as shown in Fig. 8. Figure 8(A) shows a CM waveform (from Fig. 6; probe level 75 dB SPL). Figure 8(B) shows the measured and calculated waveforms superimposed, and Fig. 8(C) shows the calculated waveform alone. Figure 8(D) shows individual components as a function of time, and Fig. 8(E) shows the same components plotted as a function of input pressure (i.e., as a transducer function). In both of these panels, the gray curves show the Boltzmann output to the combined probe-plus-bias. Panels (D) and (E) show that in addition to modulating the probe-tone response, bias-induced displacements also produce a potential change, as previously shown by the analysis presented in Fig. 7. This can be considered as the bias moving operating point up and down the Boltzmann curve, generating the potential change V_B (i.e., the voltage predicted from the Boltzmann curve), which is shown as a dotted line on both panels. The dashed line, appearing as an ellipse in Fig. 8(E) shows the additional potential V_o from Eq. (2), in this case delayed in phase by 40° with respect to the mechanical effects of the bias. This analysis suggests that the large low-frequency potentials recorded in endolymph may be accounted for by additional components that are not directly generated by the saturating transducer that the Boltzmann curve represents. The same analysis was not possible with data recorded from perilymph due to the far smaller 4.8 Hz response component in the measurement.

A summary of the most relevant parameters derived from the Boltzmann-plus-V_o [i.e., Eq. (2)] analysis of CM from the first and third cochlear turns are presented in Fig. 9. In the third turn, parameters were more dependent on probe level than in the basal turn due to the lower levels required to cause response saturation by the probe. The V_o component in the third turn was smaller than V_B with mean ratios varying from 0.3 (90 dB probe) to 0.7 (75 dB probe). This means that in the third turn, a potential with amplitude of approximately half that generated by the transducer's response to the bias may be present in the CM. In contrast, V_o was lower in the basal turn, but V_B was far lower there, so mean ratios varied from 0.3 (95 dB probe) to 2.4 (75 dB probe). Waveforms to the lower probe levels and to the no-probe condition were fitted by holding the parameters for the probe- and the bias-offset phase constant at values established with higher-level probes, showing that results with the bias alone were generally consistent with those at low-probe levels. In experiments where bias levels were varied holding probe tone level constant (Fig. 9, bottom row), both V_B and V_o components varied in a near-linear manner for both the apical and basal turns with ratios that were relatively uniform across bias level. The ratios were similar in the basal and third turns just by chance based on the choice of probe levels used as seen in the top panel. The slope parameter S_B is also

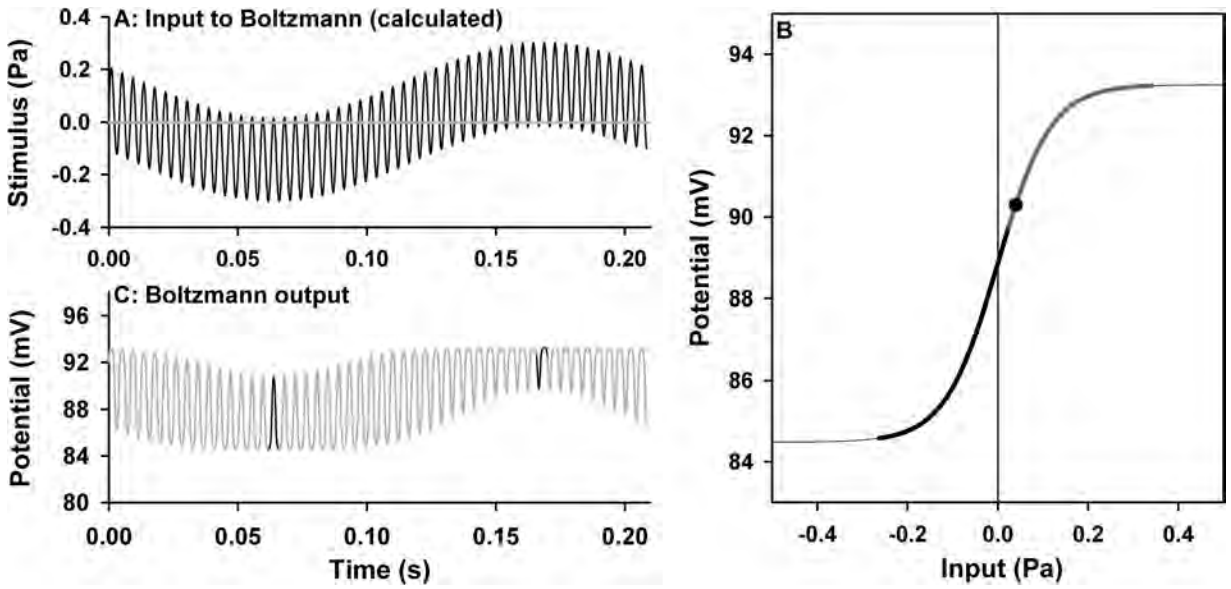

FIG. 7. (A) Combined infrasound bias plus probe stimulus combination that was the input for the calculation. The input is shown for a single cycle of the bias tone. (B) First-order Boltzmann curve relating output potential (y) to input pressure (x). A non zero operating point (black dot) is summed with the input to introduce asymmetry into the output waveform. (C) Calculated output from the Boltzmann function showing an asymmetric modulation as seen in the physiologically measured responses in Fig. 6. However, unlike the physiologically measured responses, the maximum and minimum potential from the low-frequency bias tone always coincided with the maximum degree of saturation of the probe response. This shows that a simple Boltzmann analysis cannot account for the measured response waveforms. Single cycles of the probe tone at the negative and positive limits of the bias tone are shown in (C) and are represented by the heavy gray and black lines on the curve in (B).

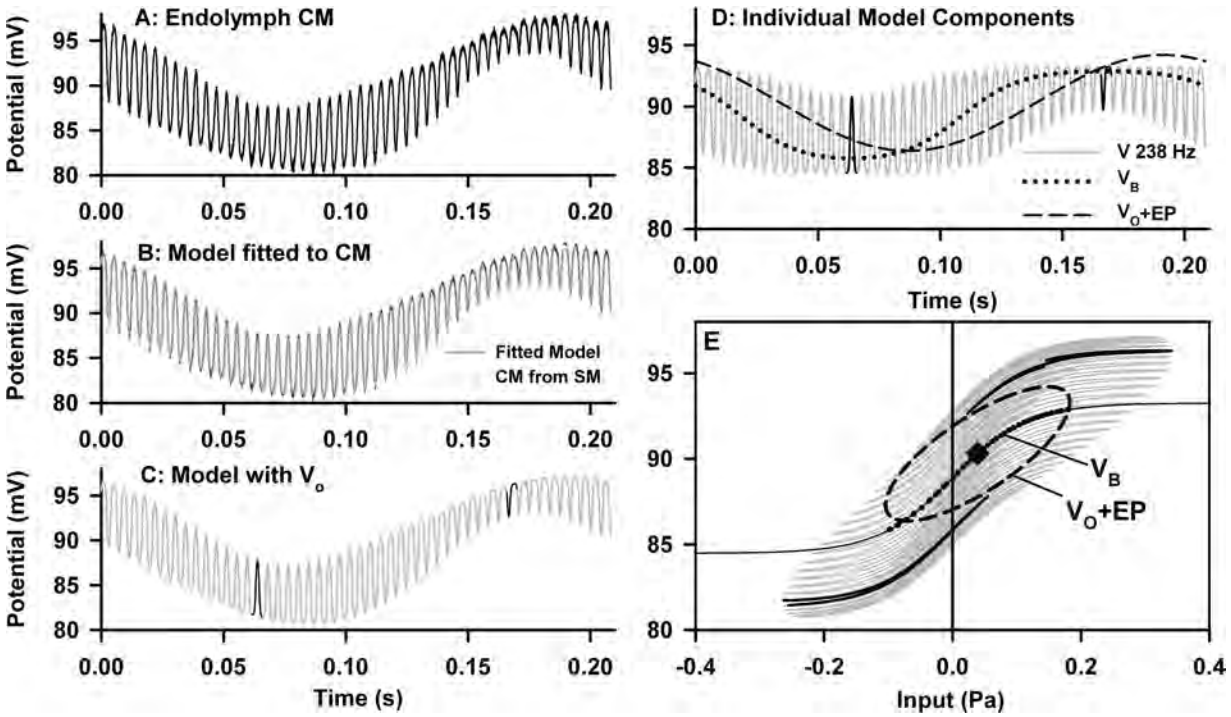

FIG. 8. Simulation in which a phase-delayed sinusoidal "offset" component (V_o) is summed with the Boltzmann output to represent the measured waveforms. (A) Physiologic data (the trace from Fig. 6 at the 75 dB probe level). (B) Calculated and measured curves overlaid showing that the analysis closely represents the measured waveform. (C) Calculated output curve with two individual cycles of the probe shown at the minimum and maximum bias pressures. (D) Components of the model, with the Boltzmann output show in gray and the phase-delayed offset component (V_o) shown dashed. A constant voltage (the EP value at the operating point) has been added to so it can be displayed in the figure. In this example, the phase delay was −40 deg. The dotted line shows the output voltage change from the bias tone displacing operating point on the Boltzmann curve (V_B). (E) Input/output relationship shown as a Boltzmann curve (thin black line) with added potential V_o + EP (dashed circle) that produces the overall the output waveform (gray lines). Single cycles of the probe at the minimum and maximum bias pressures are shown in black. The dotted line labeled V_B shows the voltage change caused by the bias tone displacing the operating point (black diamond) on the curve. This simulation illustrates that the salient characteristics of the physiologically measured waveforms are represented by this analysis.

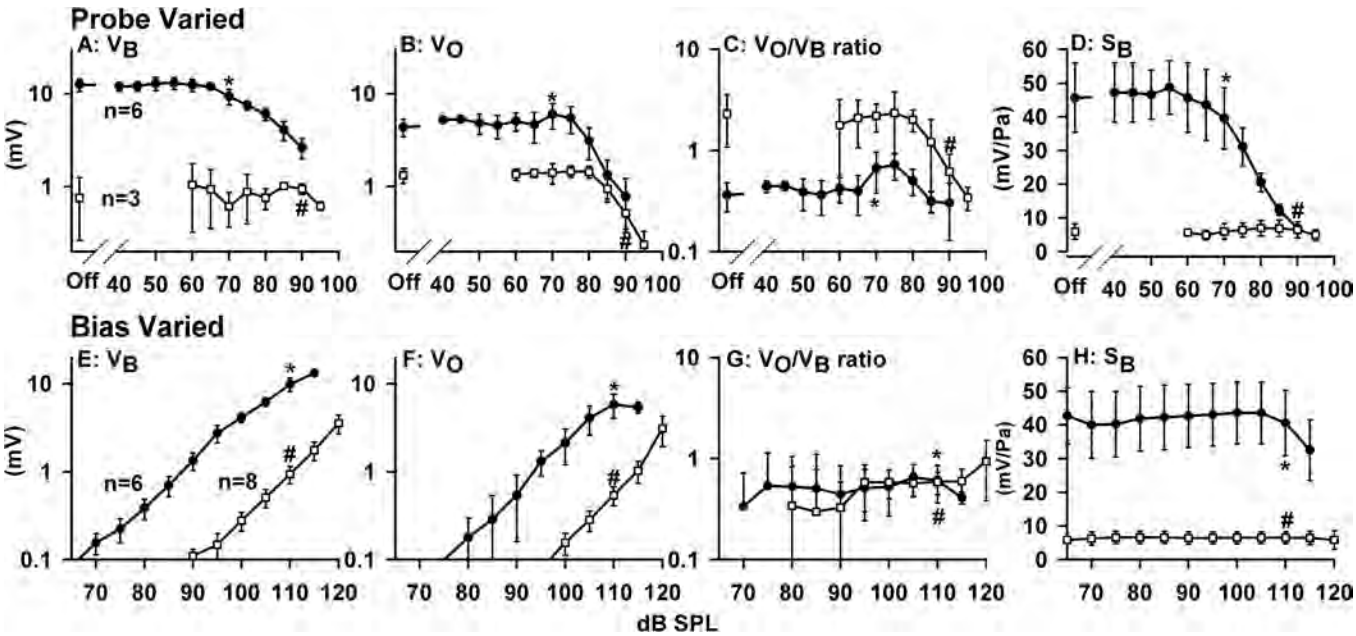

FIG. 9. Parameters derived from analysis of response waveforms recorded from the basal turn (open symbols, probe stimulus 476 Hz) and from the third turn (solid symbols, probe stimulus 238 Hz); When the probe was varied (top row), the bias level was fixed at 110 dB SPL. When the bias was varied (bottom row) the probe was set to 70 dB SPL (third turn) and 90 dB SPL (basal turn). In each row, the potential generated by the bias displacing operating point on the Boltzmann curve (V_B), the offset component (V_o) and their ratio under each condition are shown. Also shown in (D) and (H) are values of the slope parameter, S_B, that remained nearly constant for basal turn data but fell markedly as probe level was increased above 55 dB SPL for third turn data. The labels * and # represent those conditions that were replicated in both series. The number of experiments in each condition are shown on (A) and (E).

TABLE I. Average parameters derived from Boltzmann–plus-V_o waveform analysis.

	V_o phase (deg)	Bias correction (dB)	Operating point (Pa)	P_{sat} (mV)	N
		Probe varied			
Turn 3	−58.2	−33.51	0.007	5.99	38
	SD 18.0	SD 2.9	SD 0.042	SD 1.23	
Turn 1	−73.6	−42.27	−0.108	4.17	17
	SD 16.9	SD 2.7	SD 0.114	SD 0.76	
		Bias varied			
Turn 3	−61.64	−34.4	−0.002	6.11	47
	SD 22.0	SD 3.3	SD 0.02	SD 1.31	
Turn 1	−60.68	−41.02	−0.007	4.17	59
	SD 10.2	SD 3.38	SD 0.089	SD 0.53	

shown to change markedly in the third turn at higher probe levels and at the highest bias levels, while it was near constant for basal-turn data. The remaining parameters that did not vary systematically with level are shown averaged in Table I. Low probe levels (with probe varied) and low-bias levels (with bias varied) were excluded from the summary. The phase of V_o with respect to V_B averaged approximately −60 deg and was relatively consistent across all animals tested. The average bias scaling factor (S) derived from the analysis, shown in Table I in decibels, was approximately −34 dB for the third turn and −42 dB for the basal turn. These factors were derived from the waveform fitting procedure based on the amount of bias-induced displacement that accounted for the waveform shape of the response to the probe. The values were also consistent across animals and were comparable to differences in sensitivity across frequency shown for the two locations in Fig. 3.

IV. DISCUSSION

This study demonstrated that infrasound elicits larger electrical potentials in the apical regions of the cochlea than those generated by any other frequencies in the range of audibility. This confirms the existence of large endolymphatic responses seen in prior studies with low-frequency stimulation from 0.1 to 10 Hz (Salt and DeMott, 1999), although in this present study with sounds delivered acoustically via the external ear canal. The apical regions of the cochlea should therefore be regarded as highly responsive to infrasound stimulation with responses occurring at stimulus levels well below the estimated level that is perceived.

The large potentials recorded from endolymph of the third turn are locally generated and are not generated at some distant site such as the saccule. This is demonstrated by the rapid loss of responses recorded from cochlear turn 3 as KCl solution was injected at the apex. Responses to infrasound undoubtedly originate from stimulation of the OHC but are enhanced in a manner that we have quantified as an additional voltage component (V_o). CM measurements can be difficult to interpret as they are vectorally summed voltages from different regions, weighted with distance from the recording site. Gross CM measures typically do not reflect cochlear amplification because rapid frequency-dependent phase changes near the best frequency of a tone produce opposing voltages that cancel and so are not represented in the measurement (Whitfield and Ross, 1965; Cheatham and Dallos, 1982). The picture becomes simplified for CM to stimulation below the best frequency of the recording site. Phase-frequency changes are less rapid presumably because broader regions of the basilar membrane vibrate with similar phase. Phase-frequency changes are expected to be similar for infrasonic stimuli. The KCl ablation experiments (Fig. 4) show that the sites of origin of the infrasound and probe responses are similar, especially for the third turn responses. As both the infrasonic and probe stimuli are well below the best frequency of our recording site, which for the cochlear turn 3 recording site corresponds to ∼1 kHz, responses likely arise from passive cochlear mechanics.

There are a limited number of mechanisms that may give rise to V_o. If V_o arose as a dc component in the bodies of the OHCs, rather than at the mechanoelectrical transducer (MET), it would be seen in the endolymph through the resistance of the MET channels and modulated by both the probe and bias accordingly. A dc component in the OHC bodies can therefore be excluded. The IHC are also an unlikely source of V_o. Cheatham and Dallos (1994) reported that IHC dc responses were only minimally affected by a 20 Hz tone presented alone. In our measures, we found the difference between endolymph and perilymph responses increased as frequency was lowered; this is not consistent with decreasing IHC sensitivity for lower frequencies. The observation that sustained displacements of the organ of Corti by gel injection at the apex yielded V_o-like potentials when velocity and IHC stimulation would be negligible also argues against an IHC origin (Salt *et al.*, 2009). If the OHC and IHC are not the source of V_o, this leads to the possibility that non-sensory tissues of the inner ear may be contributing to the endolymphatic potentials. One possibility is that when under increased or decreased current load for a long duration, as in each half-cycle of an infrasonic stimulus, ion transport processes in the lateral wall generating EP are affected. This is comparable to a high current load on a battery causing the voltage to fall and a reduction in current load causing the voltage to rise. The possibility of changes in current drawn by the hair cells altering K^+ levels in the intrastrial space, thereby causing greater EP changes was considered in a model of EP generation (Quraishi and Raphael, 2008). Indeed, the use of low-frequency or sustained displacements of the organ of Corti to change potential in endolymph may provide a tool to evaluate the current generation capacity of stria vascularis, analogous to testing a battery by applying a high current load. This putative mechanism accounts for both the data presented here and for the large EP changes when the organ of Corti was displaced by gel injections into the apex (Salt *et al.*, 2009). Nevertheless, there may be alternative explanations if other stimulation modes of either IHCs or OHCs occur at infrasonic frequencies (Nowotny and Gummer, 2006; Guinan, 2012) or if significant potential can be generated by ion transport at other loci in the endolymphatic boundary.

The saturation, and subsequent decline, of CM growth functions with stimulus level increases (Fig. 2) has been

well-documented in classical studies although the mechanism underlying the phenomenon has not been well-described. The saturation is partly accounted for by the response characteristic of OHC that is sigmoidal and saturating with sinusoidal input. The limits of the saturating characteristics to extreme displacements represent all–channels-open and all-channels-closed—saturated states but do not explain the subsequent response decline as stimulus levels are further increased. In our analysis of waveforms, the saturating response characteristic of the Boltzmann curve is taken into account, and amplitude changes that are not accounted for by saturation are represented in the slope parameter S_B. In the fixed-bias-plus-varying-probe paradigm with low-level 238 Hz probe stimuli, S_B for third turn measurements averaged ~48 mV/Pa but declined progressively for probe levels of 60 dB and higher [Fig. 8(D)]. In contrast, in the fixed-probe-plus-varying-bias paradigm S_B was quite insensitive to the infrasonic bias level, declining only at the highest probe levels [Fig. 8(H)]. This leads us to conclude that in the absence of a probe stimulus, the endolymphatic potential in response to infrasound remains large and does not saturate because the sensitivity S_B remains high. In contrast, when a high level probe is added, S_B is reduced, which influences response amplitudes from both the probe and the bias tones. This is reflected in the suppression of the bias tone in Fig. 5 as the probe tone level is increased with the decline in bias response being accounted for by the reduction in sensitivity caused by the probe. S_B may be reduced by mechanical or electrical influences. Cooper and Rhode (1995) reported substantial two-tone suppression on the low-frequency side of the best frequency in apical mechanical measures in their study that focused quantifying the effects of a low-frequency bias tone on a higher-frequency probe rather than the effects of higher frequencies on the low-frequency bias response. In our study, one can think of this effect as the sensitivity to infrasound stimulation being maximal unless frequencies within the range of audibility are present at sufficient level to decrease the sensitivity of the *in vivo* transducer.

The endolymphatic potentials evoked by infrasound that we reported here were made through dc-coupled instrumentation and would not be detected with extracochlear recordings, such as from an electrode near the round window membrane. The response magnitude from perilymphatic sites was shown to be substantially lower and the high-pass filtering and ac coupling typically employed in extracochlear recordings would attenuate the responses further.

The EP plays a pivotal role as the battery for cochlear transduction, providing a substantial part of the electrochemical voltage driving current through the transduction channels of the hair cells. Small EP changes have been shown to substantially influence auditory sensitivity at high frequencies. A classic study by Sewell (1984) found that auditory sensitivity in cats was elevated by ~1 dB for every ~1 mV decrease in EP. Schmiedt *et al.* (2002) found a similar relationship in aged and furosemide-treated gerbil cochleae although they found far less dependence of low-frequency sensitivity on EP in higher turns that they attributed to there being less cochlear amplifier gain for low-frequency sounds. The EP changes we observed with infrasound would be expected to modulate cochlear amplifier gain for tones at their best frequency region, which would be perceived as an amplitude modulation of the tone. Biasing studies suggest the IHC respond to extracellular potentials generated by very low-frequency tones presented at high levels (Cheatham and Dallos, 1997), but the degree of sensitivity of IHC to EP and other extracellular responses to infrasonic tones (i.e., the infrasound levels at which IHC stimulation occurs) remains unknown. Objective physiologic measures of responses to low-frequency and infrasonic stimulation are not readily available. CAPs utilize onset synchrony are not sensitive indicators of low-frequency neural function but new methods, utilizing phase synchrony of low-characteristic frequency single-auditory-nerve-fibers, are becoming available to quantify apical function (Lichtenhan *et al.*, 2012). These new techniques will allow infrasound-induced modulation of neural function to be measured and compared with EP changes.

We previously estimated that with low-frequency stimulation the OHC can respond at levels as low as 40 dB below the sensitivity of the IHC; i.e., 40 dB below the threshold of hearing (Salt and Hullar, 2010). Based on the measurements in the current study, the 40 dB figure could have been an underestimate because here we have found that the apical regions of the ear are more sensitive to infrasound than we previously appreciated. We found responses to infrasound levels as low as 60–65 dB SPL (Figs. 2 and 3), in part due to the enhancement of infrasonic responses in the endolymphatic space relative to the perilymphatic space. Comparing endolymphatic potentials with hearing thresholds in guinea pigs requires consideration of the experimental conditions under which they are made. The measures were made with the auditory bulla open, the effects of which are shown to be uniform across frequency below 300 Hz but increase sensitivity by 10–15 dB (Manley and Johnstone, 1974; Wilson and Johnstone, 1975). When frequency-dependent sensitivity is considered, we would estimate that free field simulation of 70–80 dB SPL (i.e., 44–54 dB below hearing threshold) is stimulating the cochlear apical regions of the guinea pig to a degree where a 100 μV response amplitude is generated. If the human cochlea is about 15 dB more sensitive than the guinea pig, we estimate that apical regions of the human could be stimulated with 5 Hz stimulation at 55–65 dB SPL, which corresponds to −38 to −28 dBA. This estimate awaits some form of direct experimental confirmation in humans.

There is currently intense debate over whether infrasound exposure can influence human health. As wind turbines have become larger in recent years, they generate higher levels of low-frequency noise and infrasound (Møller and Pedersen, 2011). Some people who live near wind turbines report being sickened with symptoms that resolve when they move away. The wind industry generally dismisses such reports on basis that humans cannot be affected by sounds that are not heard. The present studies show that the cochlear apex is highly sensitive to low-frequency stimulation. The potentials we observed are initiated by the OHC and enhanced in the endolymphatic space by additional mechanisms, making them larger than responses to stimuli within the range of audibility. The degree of IHC stimulation caused by the changes in endolymphatic potentials remains uncertain. A scientific conundrum remains

over why the cochlea would transduce such sounds and generate large potentials and then discard this information from conscious hearing. The answer may be that the majority of low-frequency sound is unwanted noise, such as from respiration, heartbeat, head movements, etc. There may be mechanisms present both to transduce the sound and then cancel it from conscious hearing (analogous to a noise-canceling headphone). Neural pathways exist from the OHC to the cochlear nucleus, which are potentially inhibitory to hearing (Kaltenbach and Godfrey, 2008) and could suppress perception of responses mediated by the IHC. Although there is clearly a need to understand how the ear responds to low-frequency sounds in more detail and how it affects the body as a whole, the present study confirms that the inner ear is highly sensitive to infrasonic and low-frequency stimulation. It seems unreasonable to believe that infrasound cannot influence the animal or person when it generates such large endolymphatic potentials.

Alves-Pereira, M., and Castelo Branco, N. A. (**2007**). "Vibroacoustic disease: Biological effects of infrasound and low-frequency noise explained by mechanotransduction cellular signaling," Prog. Biophys. Mol. Biol. **93**, 256–279.

Broner, N. (**2008**). "Effects of infrasound, low-frequency noise and ultrasound on people," in *Handbook of Noise and Vibration Control*, edited by M. J. Crocker (Wiley and Sons, Hoboken, NJ), pp. 320–325.

Brown, D. J., Hartsock, J. J., Gill, R. M., Fitzgerald, H. E., and Salt, A. N. (**2009**). "Estimating the operating point of the cochlear transducer using low-frequency biased distortion products," J. Acoust. Soc. Am. **125**, 2129–2145.

Cheatham, M. A., and Dallos, P. (**1982**). "Two-tone interactions in the cochlear microphonic," Hear. Res. **8**, 29–48.

Cheatham, M. A., and Dallos, P. (**1994**). "Stimulus biasing: A comparison between cochlear hair cell and organ of Corti response patterns," Hear. Res. **75**, 103–113.

Cheatham, M. A., and Dallos, P. (**1997**). "Low-frequency modulation of inner hair cell and organ of Corti responses in the guinea pig cochlea," Hear. Res. **108**, 191–212.

Cheatham, M. A., and Dallos, P. (**2001**). "Inner hair cell response patterns: Implications for low-frequency hearing," J. Acoust. Soc. Am. **110**, 2034–2044.

Cooper, N. P., and Rhode, W. S. (**1995**). "Nonlinear mechanics at the apex of the guinea-pig cochlea," Hear. Res. **82**, 225–243.

Dallos, P. (**1970**). "Low-frequency auditory characteristics: Species dependence," J. Acoust. Soc. Am. **48**, 489–499.

Dallos, P. (**1973**). *The Auditory Periphery* (Academic, New York), pp. 228–246.

Dallos, P. (**1986**). "Neurobiology if cochlear inner and outer hair cells: Intracellular recordings," Hear. Res. **22**, 185–198.

Dallos, P., Santos-Sacchi, J., and Flock, Å. (**1982**). "Intracellular recordings from cochlear outer hair cells," Science **218**, 582–584.

Echteler, S. M., Fay, R. R., and Popper, A. N. (**1994**). "The influence of cochlear shape on low frequency hearing," in *Comparative Hearing: Mammals*, edited by R. R. Fay and A. N. Popper (Springer, New York), pp. 134–171.

Franke, R., and Dancer, A. (**1982**). "Cochlear mechanisms at low frequencies in the guinea pig," Arch. Otorhinolaryngol. **234**, 213–218.

Guinan, J. J., Jr. (**2012**). "How are inner hair cells stimulated? Evidence for multiple mechanical drives," Hear. Res. **292**, 35–50.

Heffner, R., Heffner, H., and Masterton, B. (**1971**). "Behavioral measurements of absolute and frequency-difference thresholds in guinea pig," J. Acoust. Soc. Am. **49**, 1888–1895.

Honrubia, V., Strelioff, D., and Ward, P. H. (**1973**). "A quantitative study of cochlear potentials along the scala media of the guinea pig," J. Acoust. Soc. Am. **54**, 600–609.

Honrubia, V., and Ward, P. H. (**1968**). "Longitudinal distribution of the cochlear microphonics inside the cochlear duct (guinea pig)," J. Acoust. Soc. Am. **44**, 951–958.

ISO (**1996**). 7196, *Acoustics—Frequency-Weighting Characteristic for Infrasound Measurements* (International Organization for Standardization, Geneva, Switzerland).

Jakobsen, J. (**2005**). "Infrasound emission from wind turbines," J. Low Freq. Noise Vib. Active Control **24**, 145–155.

Kaltenbach, J. A., and Godfrey, D. A. (**2008**). "Dorsal cochlear nucleus hyperactivity and tinnitus: Are they related?," Am. J. Audiol. **17**, S148–S161.

Lichtenhan, J. T., Cooper, N. P., and Guinan, J. J. (**2012**). "A new auditory threshold estimation technique for low frequencies: Proof of concept," Ear Hear. **34**, 42–51.

Manley, G. A., and Johnstone, B. M. (**1974**). "Middle-ear function in the guinea pig," J. Acoust. Soc. Am. **56**, 571–576.

Miller, J. D., and Murray, F. S. (**1966**). "Guinea pig's immobility response to sound: Threshold and habituation," J. Comp. Physiol. Psychol. **61**, 227–233.

Møller, H., and Pederson, C. S. (**2004**). "Hearing at low and infrasonic frequencies," Noise Health **6**, 37–57.

Møller, H., and Pedersen, C. S. (**2011**). "Low-frequency noise from large wind turbines," J. Acoust. Soc. Am. **129**, 3727–3744.

Nowotny, M., and Gummer, A. W. (**2006**). "Nanomechanics of the subtectorial space caused by electromechanics of cochlear outer hair cells," Proc. Natl. Acad. Sci. USA **103**, 2120–2125.

O'Neal, R. D., Hellweg, R. D., Jr., and Lampeter, R.M. (**2011**). "Low frequency noise and infrasound from wind turbines," Noise Control Eng. J. **59**, 135–157.

Patuzzi, R., and Moleirinho, A. (**1998**). "Automatic monitoring of mechano-electrical transduction in the guinea pig cochlea," Hear. Res. **125**, 1–16.

Prosen, C. A., Petersen, M. R., Moody, D. B., and Stebbins, W. C. (**1978**). "Auditory thresholds and kanamycin-induced hearing loss in the guinea pig assessed by a positive reinforcement procedure," J. Acoust. Soc. Am. **63**, 559–566.

Quraishi, I. H., and Raphael, R. M. (**2008**). "Generation of the endocochlear potential: A biophysical model," Biophys. J. **94**, L64–66.

Salt, A. N., Brown, D. J., Hartsock, J. J., and Plontke, S. K. (**2009**). "Displacements of the organ of Corti by gel injections into the cochlear apex," Hear. Res. **250**, 63–75.

Salt, A. N., and DeMott, J. E. (**1999**). "Longitudinal endolymph movements and endocochlear potential changes induced by stimulation at infrasonic frequencies," J. Acoust. Soc. Am. **106**, 847–856.

Salt, A. N., and Hullar, T. E. (**2010**). "Responses of the ear to low frequency sounds, infrasound and wind turbines," Hear. Res. **268**, 12–21.

Schmiedt, R. A., Lang, H., Okamura, H. O., and Schulte, B. A. (**2002**). "Effects of furosemide applied chronically to the round window: A model of metabolic presbyacusis," J. Neurosci. **22**, 9643–9650.

Sewell, W. F. (**1984**). "The effects of furosemide on the endocochlear potential and auditory-nerve fiber tuning curves in cats," Hear. Res. **14**, 305–314.

Sirjani, D. B., Salt, A. N., Gill, R. M., and Hale, S. A. (**2004**). "The influence of transducer operating point on distortion generation in the cochlea," J. Acoust. Soc. Am. **115**, 1219–1229.

Van den Berg, G. P. (**2006**). "The sound of high winds: The effect of atmospheric stability on wind turbine sound and microphone noise," Ph.D. dissertation, University of Groningen, Netherlands. http://dissertations.ub.rug.nl/faculties/science/2006/g.p.van.den.berg/ (Last viewed 8/3/2012).

von Békésy, G. (**1951**). "Microphonics produced by touching the cochlear partition with a vibrating electrode," J. Acoust. Soc. Am. **23**, 18–28.

von Békésy, G. (**1960**). *Experiments in Hearing* (McGraw-Hill, New York), pp. 672–682.

Walloch, R. A., and Taylor-Spikes, M. (**1976**). "Auditory thresholds in the guinea pig: A preliminary report of a behavioral technique employing a food reward," Laryngoscope **86**, 1699–1705.

West, C. D. (**1985**). "The relationship of the spiral turns of the cochlea and the length of the basilar membrane to the range of audible frequencies in ground dwelling mammals," J. Acoust. Soc. Am. **77**, 1091–1101.

Whitfield, I. C., and Ross, H. F. (**1965**). "Cochlear microphonic and summating potentials and the outputs of individual hair cell generators," J. Acoust. Soc. Am. **18**, 401–408.

Wilson, J. P., and Johnstone, J. R. (**1975**). "Basilar membrane and middle-ear vibration in guinea pig measured by capacitive probe," J. Acoust. Soc. Am. **57**, 705–723.

THIS PAGE INTENTIONALLY LEFT BLANK.